Applied Thermal Engineering 280 (2025) 128222

Contents lists available at ScienceDirect

Applied Thermal Engineering

journal homepage: www.elsevier.com/locate/apthermeng

A review of photovoltaic cooling with phase change materials: Technical advances, modeling approaches, efficiency gains and economic/environmental impact☆

Domenico Mazzeo *, Luigi Pietro Maria Colombo, Sonia Leva

Politecnico di Milano, Department of Energy, Via Lambruschini 4a, 20156 Milan, Italy

ARTICLE INFO

Keywords:
Photovoltaic systems
Phase change materials
Thermal regulation
Solar energy efficiency
Cooling technologies
Renewable energy systems

ABSTRACT

The integration of phase change materials (PCMs) with photovoltaic (PV) modules is a promising solution to mitigate thermal losses and enhance solar energy efficiency. Given the substantial heat generated during PV operation, especially in hot climates, effective passive thermal regulation using PCMs is crucial for optimal performance. This review synthesizes PCM-based cooling strategies, detailing material properties, applications, and performance benefits, including temperature reduction and energy efficiency gains. Unlike prior surveys, this review integrates materials, modeling and validation, and techno-economic/environmental evidence with a comprehensive literature matrix and scientometric analysis, making the contribution and scope explicit for readers and practitioners. A range of organic, inorganic, and eutectic PCMs is reviewed, each with specific benefits tied to phase transition properties. Notably, advanced solutions such as PCM nanoparticles, porous metal foams, and hybrid PV/T-PCM configurations are examined. Enhancements like nanoparticles and metal foams improve conductivity, while hybrid PV/T-PCM systems deliver added thermal and electrical gains. Cycling-stability evidence is summarized, and design/packaging guidance to mitigate degradation in long-term PV–PCM operation is provided. The review also includes simplified and detailed coupled thermal-electrical models and discusses limits, computational cost, and use cases to guide model choice. A literature matrix summarizes key studies, comparing geographic location, analysis period, thermophysical and electrical characteristics, integration methods, and types of analysis (experimental or numerical), along with parametric, energy, economic, and environmental evaluations. A global scientometric survey (2003–2025) quantifies research trends and regional focus. The matrix highlights significant reductions in module temperature and improvements in output and efficiency. Findings show that PCMs can lower PV temperatures by up to 30 °C and boost efficiency by 1–14 %. Comparative studies confirm the viability of PV-PCM systems across diverse climates, highlighting their techno-economic performance and sustainability benefits. Climate-based analysis suggests PV-PCM systems are most effective in hot, arid zones, though cost-effectiveness varies. Overall, this comprehensive review outlines the progress, key challenges, and future opportunities in PV-PCM integration, stressing material optimization, cost reduction, and long-term performance evaluation.

1. Introduction

The control of operating temperature in photovoltaic (PV) modules has become a key focus in solar energy research, as PV performance, particularly efficiency and electrical output, is highly sensitive to factors like solar irradiance on the module surface, PV temperature, surface thermal losses, and material technology [1]. Studies have shown that typical PV arrays convert only 5 %–25 % of incident solar irradiance into electrical energy [2], while the remainder is dissipated as heat [3–5].

It is well-documented that elevated operating temperatures result in marked reductions in electrical output from PV modules. For silicon-based PVs, operating above 25 °C induces a temperature-dependent power decline, with temperature coefficients ranging from −0.3 % $°C^{-1}$ to −0.65 % $°C^{-1}$, varying by module type and manufacturing technology [6–8]. In extreme cases, such as in southern Libya in 2007, PV modules reached temperatures of 125 °C, leading to a severe 69 %

☆ This article is part of a special issue entitled: 'Cold Storage & Cooling Systems' published in Applied Thermal Engineering.

* Corresponding author.
E-mail address: domenico.mazzeo@polimi.it (D. Mazzeo).

https://doi.org/10.1016/j.applthermaleng.2025.128222
Received 22 May 2025; Received in revised form 16 August 2025; Accepted 3 September 2025
Available online 6 September 2025

reduction in power output relative to nominal values [9].

PV manufacturers generally recommend operating temperature ranges of −40 °C to 85 °C. However, in hot and arid climates, module temperatures frequently exceed these limits, which can lead to power losses, accelerated degradation, and potential cell delamination [10]. Consequently, effective cooling strategies are essential to maintaining and enhancing PV efficiency. These cooling methods are classified as either active technologies, which rely on induced air or water flow, or passive technologies, which act as heat sinks to absorb excess heat from the modules [11].

Active cooling systems for PV modules, widely studied for their effectiveness in temperature regulation, typically employ pumps, fans, or other technologies to direct water or air across the PV module's front or back surfaces, thereby enhancing heat dissipation rates. This approach has been shown to improve PV performance beyond what passive cooling can achieve, although it incurs additional power consumption and maintenance costs [11]. However, if the thermal energy generated can be repurposed, such as for building applications, active cooling can offset some of these capital expenses and become more cost-effective [11].

Water-based active cooling systems: numerous water-based active cooling models have been tested. For instance, the Department of Physics at the Federal State University of Ceará (UECE) developed a system where a thin water film flows over the PV module's front surface [12]. This design not only maintains module cleanliness but also reduces reflection by 2 %-3.6 % and lowers module temperature by up to 22 °C, leading to an increase in conversion efficiency. Over a full day, the system achieved a 10.3 % gain in electrical energy yield. When accounting for the energy consumed by a high-efficiency pump necessary to sustain water flow, the net benefit of the system was estimated to be around 8 %-9% [12].

Another innovative approach, developed by the School of Engineering at the University of Technology, Jamaica (UTech), replaced conventional pumping with a gravity-fed water system that flows across the back of the PV module. Experimental results demonstrated that this technique mitigates the adverse effects of high cell temperatures on the open-circuit voltage, thereby enhancing power output without requiring an active pump. Utilizing the hydraulic head from an upstream reservoir, this design stabilizes the module temperature, reducing PV cell temperatures from 62 °C to 30 °C and yielding a 12.8 % improvement in conversion efficiency [13].

In addition, the Department of Mechanical and Electrical Engineering at Yatsushiro National College of Technology advanced a pump-free cooling system, utilizing siphonage and incorporating a mechanism for reusing the heated water from the cooling process. This system confirmed that active cooling without auxiliary energy-intensive components can positively impact PV electricity production [14].

Air-based active cooling systems: air-based active cooling represents another effective method for thermal regulation in PV systems, offering fewer constraints compared to buoyancy-driven natural airflow [11]. Tonui et al. [15,16] designed an air collector positioned at the rear of the module, where fans or air pumps circulate air within channels or promote natural convection. This airflow absorbs the PV module's excess heat, and heat dissipation is further enhanced through the addition of finned profiles, corrugated metal sheets, or wire mesh within the air channels [15]. Experimental applications of air circulation have been shown to reduce PV temperature by at least 5 °C, leading to a corresponding increase in electrical efficiency [16]. Notably, this approach can be integrated into building facades or roofs using low-cost materials, making it a cost-effective and adaptable solution for practical implementation [15].

Further research on air-filled asymmetric compound parabolic PV concentrators (ACPPVCs) has used a unified model combining optics and heat transfer for line-axis solar energy systems. Simulations investigated the influence of inlet air velocity and air channel dimensions on the PV module's front and back temperatures. A reduction of up to 34.2 °C was projected with an inlet air velocity of 1 m/s and 20 mm air gaps at the front and back, showcasing the potential of advanced air-cooling designs for effective temperature management [17].

Passive cooling for PV systems, which leverages convection, conduction, and radiation, is commonly implemented to dissipate heat without requiring external energy input. Typically, a duct or air channel located behind the PV module or mounting system facilitates heat removal through buoyancy-driven airflow, or natural circulation, as heated air rises due to the module's rear heat transfer [11].

In building-integrated PV installations, this cooling technique is widely applied, with PV modules positioned on building facades or roofs and air allowed to flow in a channel between the back of the modules and the building's wall. Studies have shown that duct depth is critical, especially when wall temperatures peak and impact array efficiency. For optimal heat dissipation, a duct with length L that allows fully developed flow achieves ideal cooling at a ratio of L/D (length to hydraulic diameter) near 20, a value that remains stable across varying conditions and inclination angles, making it suitable for most vertical or sloped installations [18–20].

A more advanced passive cooling method, as explored by Sargunanathan et al. [21], involves a heat pipe, a device designed for efficient thermal management via a two-phase flow of a working fluid. The heat pipe consists of three sections, an evaporator, an adiabatic zone, and a condenser, and is filled with a working fluid under vacuum; the evaporator, typically attached to the rear of PV cells, absorbs heat and causes the fluid to vaporize. This vapor, carrying latent heat, travels to the condenser section, where it releases heat through natural convection and condenses back into liquid. Heat pipes are generally made from materials such as copper and aluminum, chosen for their compatibility and efficiency within a temperature range of 20 °C to 100 °C [21].

Akbarzadeh and Wadowski [22] introduced a passive thermosyphon-based cooling system consisting of two heat exchangers linked by a pipe. This system uses R11 as a working fluid, which undergoes evaporation and condensation to transfer heat from the solar cells. In this setup, the lower heat exchanger, acting as an evaporator, absorbs heat from the PV module, causing the liquid R11 to vaporize and move to the upper heat exchanger, or condenser, where it condenses with external cooling. Gravity returns the liquid to the evaporator, completing the cycle. This system reduced PV temperature from 84 °C to 46 °C, improving power output from 10.6 W to 20.6 W [22].

Additional passive cooling methods involve heat sinks or aluminum fin profiles mounted on the back of PV panels. These enhance thermal dissipation by maximizing the heat transfer coefficient, often with a thin layer of thermally conductive paste. This technique has proven effective, increasing energy efficiency by up to 9 % with heat sinks and 1.8 % with fins [21,23].

Earlier surveys emphasized PV–PCM technology status, materials selection, and PV/T cooling families, often without a unified discussion of model validation, safety/aging, or climate-aware temperature selection. For example, Waqas et al. synthesize PV–PCM development, performance ranges, and mass/area guidelines [24]; Preet reviews both water-based PV/T and PV–PCM cooling arrangements and flags low conductivity and nocturnal solidification [25]; Ma et al. center on materials selection and define PV–PCM scope and energy-balance analysis [26]. Our contribution complements these by integrating materials, integration, modeling/validation, safety/aging, techno-economics, and by adding a literature matrix and scientometric analysis (2003–2025) to support design-oriented synthesis.

As highlighted in Table 1, unlike previous reviews, this paper uniquely combines PCM material taxonomy, hybrid system designs, thermal–electrical modeling, and global techno-economic analysis with a literature matrix and scientometric evaluation. In addition, we synthesize validation practices for models, safety, and cycling stability (packaging, flammability, aging), and climate-aware selection of phase-change temperature to provide actionable guidance for PV–PCM design and assessment. The review focuses on PV modules passively cooled by

Table 1
This review compared to representative prior surveys of PV cooling with PCMs.

Review (year)	Time span/ corpus	Primary focus	Distinctive emphases & key quantitative takeaways	What was *not* covered in depth
Waqas et al. [24], RSER 92 (2018) — *Thermal and electrical management of PV panels using PCMs: a review*	Up to 2017; PV-PCM cooling	Broad technology status: system development, PCM selection, heat-transfer enhancement, simulation, costs	Reports PV peak temperature reduction up to 20 °C and efficiency increase up to ~ 5 %; cites ≈2.6 kg PCM·m^{-2} per 1 °C drop as a heuristic; highlights R&D status and cost barriers.	Model validation practices; fire/cycling durability synthesis; scientometrics/ literature matrix
Preet [25], RSER 82 (2018) — *Water and PCM-based PV/T management: a review*	Up to 2017; PV/T (water/air) + PV-PCM	Typology of PV/T and PV-PCM; equations/metrics; component-level issues	Flags low conductivity and nocturnal solidification as core PCM challenges; proposes heat-transfer elements and heat extraction to regulate PCM temperature; details PV/T classifications.	Materials taxonomy depth; climate-aware temperature selection; validation + safety integration
Ma et al. [26], RSER 116 (2019) — *PV-PCM: technology overview and materials selection*	104 articles (2004–2018)	Materials selection and PV-PCM definition/scope; system configuration; energy balance	Proposes selection criteria and a strategy for phase-transition temperature; frames PV-PCM vs. PV/T and outlines development stages.	Validation protocols; fire risk and cycling degradation; scientometric mapping to 2025

PCMs (including shape-stabilized and encapsulated forms), covers experimental and modeling studies across climates, and reports performance using consistent indicators (ΔT, efficiency gain as percentage points, and percent).

The paper is organized as follows. Section 2 outlines PCM cooling fundamentals and integration routes. Section 3 surveys recent PV–PCM literature and presents the scientometric mapping and literature matrix. Section 4 develops detailed and reduced-order thermal–electrical PV–PCM models, states their assumptions, and consolidates performance indicators. Section 5 examines cycling stability/degradation and safety (including fire-risk mitigation), and summarizes integration practices. Section 6 synthesizes major findings from representative studies. Section 7 assesses environmental and techno-economic evidence on PV–PCM systems. Section 8 concludes with implications and future research directions.

2. PCM cooling

Phase change materials (PCMs) provide an effective cooling solution for PV modules by absorbing excess heat generated during module operation. This approach stands out among thermal regulation techniques due to PCMs' substantial phase change enthalpy, ease of implementation, cost-effectiveness, chemical stability, and customizable phase transition temperatures [27]. These advantageous properties have led to the extensive use of PCMs across diverse temperature regulation applications in engineering, including electronic cooling, automotive systems, solar thermal energy applications, and heat recovery systems [28–30].

In PV cooling applications, PCMs can be deployed as standalone systems or integrated into hybrid PV/thermal (PV/T) systems to allow simultaneous generation of hot water for auxiliary uses. Enhancements to PCM-based cooling can be achieved by incorporating fins, adding nanoparticles, or embedding porous metal foams, which effectively increase the heat transfer surface area and boost thermal conductivity [31]. Typically, PCMs are placed on the rear of PV modules (illustrated in Fig. 1), where they dissipate solar thermal energy, thereby maintaining a stable and uniform operating temperature across the PV cells for extended periods [32].

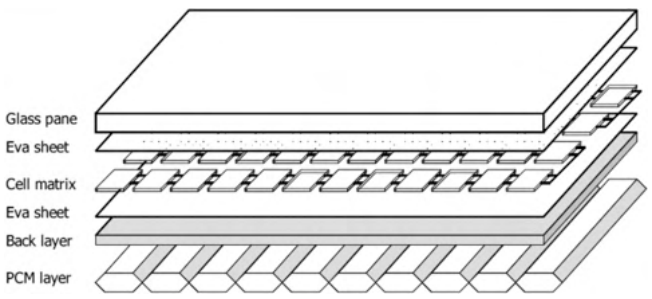

Fig. 1. Typical structure of a PV-PCM system.

Thermal dissipation occurs through two different physical phenomena: initially, the PCM absorbs excess heat from the module as sensible heat until it reaches the phase-change temperature, then the dissipation continues through latent heat exchange until the PCM is completely melted. This mechanism helps cool solar cells, thereby increasing the power output of the PV module [31]. During sunless hours, the heat absorbed by the PCM is released into the environment, lowering the PCM temperature and allowing it to solidify. This cycle repeats the following morning when cooling resumes [31].

2.1. PCM properties

In a study conducted by Hasan et al. [33], five distinct types of PCMs, encompassing both organic and inorganic varieties, were evaluated based on their melting points, which ranged from 21 to 30 °C, and latent heat values spanning from 170 to 240 kJ/kg. The results indicated that certain materials failed to release heat effectively during the discharging phase due to excessively low freezing temperatures, whereas others exhibited superior performance in both charging and discharging processes [33].

Consequently, the selection of an appropriate PCM for cooling solar cells is of paramount importance and is influenced by both the melting point and the ambient temperature. Practically, the phase-change temperature should be selected so that typical midday PV back-surface temperatures lie ~ 5–15 °C above it, while night-time minima fall ≥ 5–10 °C below it in the target season. Hasan et al. [33] outlined the necessary properties of PCMs, categorizing them into thermal, physical, kinetic, chemical, economic, and environmental properties, each of which plays a vital role in optimizing the efficiency and safety of PCMs in practical applications.

i. Thermal properties: high latent heat and effective heat capacity are essential for maximizing heat absorption and minimizing sensible heating, thereby enhancing the PCM's efficiency in thermal transfer. Adequate thermal conductivity is also critical for effective heat removal, while a stable melting point and reversible phase change ensure consistent and cyclical thermal responses, particularly in diurnal applications.
ii. Physical properties: congruent melting is beneficial for minimizing thermal gradients, while low volumetric expansion reduces the potential for overdesign issues. High density aids in reducing containment requirements, resulting in more practical and compact storage solutions.
iii. Kinetic properties: the absence of supercooling facilitates the freezing process, and a favorable crystallization rate enables rapid solidification, thereby improving performance in dynamic applications.

iv. Chemical properties: chemical stability and non-corrosiveness contribute to the longevity of the PCM and its containment, while non-flammable and non-explosive characteristics ensure compliance with safety regulations, making the PCM suitable for various building applications. Additionally, non-toxic attributes further enhance safety for users.
v. Economic properties: the abundance and cost-effectiveness of PCMs are critical for their economic viability and competitiveness in the market, promoting broader adoption and penetration.
vi. Environmental properties: the recyclability and reusability of PCMs support environmentally responsible disposal methods and reduce overall environmental impact. Additionally, being odor-free makes these materials suitable for residential applications.

This comprehensive set of requirements is designed to ensure that PCMs fulfill performance, safety, and sustainability standards across a wide range of applications.

2.2. PCM integrated with PV systems

In a practical experiment conducted by Hasan et al. [34], which spanned all four seasons, the use of paraffin wax as a PCM with a melting point between 38 and 43 °C was evaluated when installed on the rear side of a PV module. The findings indicated optimal performance during the autumn and spring seasons, as the moderate ambient temperatures facilitated the complete melting of the PCM during daylight hours and solidification at night. However, during the summer months, elevated temperatures inhibited the complete solidification of the PCM, while winter temperatures were insufficient to fully melt the PCM. Overall, the integration of the PV-PCM system resulted in a 5 % increase in energy output compared to a PV module without PCM [34]. Some of the previous authors conducted a comparative analysis of two distinct PCM cooling systems: capric-palmitic acid and calcium chloride hexahydrate ($CaCl_2{\cdot}6H_2O$), across warmer and cooler climates [35]. In cooler conditions, the results demonstrated that the application of the two PCMs reduced the temperatures of the PV modules from 49 °C to 43 °C and 40 °C, respectively. Conversely, in warmer climates, the temperature reductions observed were from 63 °C to 51 °C for capric-palmitic acid and to 42 °C for $CaCl_2{\cdot}6H_2O$, thereby underscoring the economic viability of PCM cooling systems in hotter environments.

An experiment conducted by Stropnik and Stritih [36] utilized RT28 as a PCM, with results indicating an increase in power output from 4.3 % to 8.7 % relative to an unmodified PV module. Hachem et al. [37] investigated the cooling efficacy of a PV module utilizing a PCM comprised of white petroleum jelly against a PCM consisting of a mixture of white petroleum jelly, copper, and graphite. The composite PCM exhibited a 5.5 % enhancement in electrical efficiency, compared to a 3 % improvement observed with the sole use of white petroleum jelly.

Moreover, Hasan et al. [38] proposed the integration of PCMs into building-integrated PV systems, which resulted in a temperature reduction of 21.8 °C and a corresponding increase in electrical efficiency of 7.3 %.

2.3. PCM integrated with PV/T thermal system

In an experiment conducted by Fayaz et al., an integrated PCM system combined with a PV/T system was evaluated against a standard PV/T system and a conventional PV module [39]. The findings revealed that the PV/T-PCM system achieved an electrical efficiency of 12.75 %, whereas the electrical efficiencies for the standard PV module and the standard PV/T system were recorded at 11.35 % and 12.4 %, respectively.

Browne et al. investigated the use of a palmitic acid/capric acid mixture as a PCM integrated into a PV/T system [40]. Their results indicated that this PCM integration led to a temperature reduction of 5 °C compared to a PV/T system that did not incorporate a PCM.

Hassan et al. reported a significant increase in electrical efficiency of 23.9 % for a PV module utilizing a cooling system, compared to 22.7 % increase observed with a standard PV/T cooling system [41].

2.4. PCM with additives

Despite the promising characteristics of PCMs, including high energy density and compact storage volume, their low thermal conductivity poses a significant challenge, reducing the effectiveness of heat exchange during both the charging and discharging phases [42]. To mitigate this limitation, various strategies have been investigated to enhance the thermal conductivity of PCMs, thereby improving their overall performance.

PCM containers with fins: an experiment conducted by Tan et al. [43] demonstrated that incorporating fins within the PCM in direct contact with the PV module resulted in a maximum temperature reduction of 16 °C, which corresponded to a 5.9 % increase in PV efficiency. Kumar et al. [44] further illustrated this concept through an experiment involving three PV systems, each equipped with a container filled with PCM and external fins. The findings indicated that a temperature reduction of 22 °C was achievable, compared to an 11.3 °C decrease observed in a conventional container. Consequently, the integration of fins to enhance heat transfer between the PV system and the PCM has proven effective in improving the performance of cooling systems, with an increased number of fins correlating to greater effectiveness [45].

PCM with nanoparticles: numerous studies have explored the incorporation of nanoparticles into PCMs to improve their thermal conductivity. In an experiment by Nada et al., a PV system utilizing PCM mixed with Al_2O_3 nanoparticles was compared to a standard PV module and a module paired with pure PCM [46]. The results indicated that the PCM with nanoparticles achieved a 13.2 % increase in electrical efficiency relative to the standard PV system, whereas pure PCM alone yielded a 5.7 % efficiency improvement. Additionally, an experiment by Al-Waeli et al. aimed to enhance the performance of a PV/T system by introducing a nanofluid to the water and SiC nanoparticles to the PCM [47]. The findings revealed an increase in electrical efficiency ranging from 7.1 % to 13.7 %, with thermal efficiency reaching 72 %. Similarly, the addition of CuO nanoparticles to PCM resulted in a 6.5 % increase in power output [48].

PCM with porous metal: a study by Duan and Li [49] found that the heat transfer capability of a PCM integrated with a porous metal foam system is ten times greater than that of a pure PCM system. Furthermore, the presence of metal foams within the PCM contributed to enhanced temperature uniformity and significantly reduced melting time [50,51]. In an experiment conducted by Abdulmunem et al., a PCM integrated with a copper foam matrix was compared to a PV system without PCM and to a system using pure PCM [52]. The results showed a 5.68 % increase in electrical efficiency relative to the standard module, and a 1.97 % increase over the system utilizing pure PCM. Rad et al. demonstrated that the incorporation of aluminum shavings as a porous material within the PCM, particularly under hot climatic conditions, could achieve a temperature reduction of up to 24 °C, resulting in a 2.5 % increase in electrical efficiency [53]. A numerical investigation by Klemm et al. further indicated that the use of metal fibers within the PCM for passive cooling of PV modules can lead to a temperature reduction of 21 °C, with porosity having minimal impact on the performance of this system [54].

3. Literature overview and scientometric review

This section provides a comprehensive analysis of the most pertinent literature from the last decade, which is summarized in the literature matrix presented in Table 2 [1,34–37,55–73].

The primary database was Scopus, cross-checked in Web of Science

Core Collection to avoid omissions. The Boolean query was (photovoltaic AND phase AND change AND material AND cooling), limited to recent English-language records and last updated on 20 May 2025. We included studies on PV modules passively cooled by PCMs (macro/micro/shape-stabilized) reporting at least one outcome among ΔT, efficiency, or energy yield with sufficient methodological detail. We excluded active-only PV/T without PCM, thermal storage with no PV coupling, non-electrical solar applications, duplicates, non-English records, and items with insufficient outcome data for extraction. From the scientometric corpus, a curated subset of 24 studies was extracted into Table 2 for side-by-side comparison of thermophysical properties, integration method, climate/site, and outcomes.

For each included matrix study, the following information was extracted: PV technology and nominal power; PCM type and phase-change temperature, latent heat, and conductivities; encapsulation/coupling method; Köppen–Geiger climate class/site; and results/indicators (ΔT, η_{PV} and η_{PV-PCM} in %, Δη in percentage points, energy/EEP %, plus parametric, energy, economic, and environmental evaluations), as reported in Table 2.

Key takeaways. (i) Most experimental ΔT values cluster around 10–30 °C, with upper-end performance in arid sites; (ii) typical electrical gains are 1–5 %, with occasional double-digit outliers tied to strong daily activation; (iii) studies that match the phase-change temperature to local climate report more consistent gains and better overnight reset.

Table 2 provides a comprehensive summary of the most relevant studies examining the integration of PCMs with PV systems. It includes pertinent details regarding the types of PV modules employed, the properties of the PCMs, the methods of coupling, the geographical locations of the studies, and the key findings reported. The literature indicates that the topic of PV-PCM systems is relatively recent, with the first relevant study published in 2014 [35]. A thorough exploration of the most relevant articles related to this work has been conducted,

Table 2
Literature matrix of the main relevant publications in the PV-PCM research field. Photovoltaic module type and rating, PCM type and thermophysical properties, coupling/integration, study location, and analysis type are reported. Derived performance metrics are added where available: ΔT (°C) = back-surface temperature drop, Δη (pp) = absolute efficiency gain (percentage points), and/or EEP (%) = enhancement in electrical efficiency, and ΔE (%) = energy gain (power enhancement percentage PEP calculated in energy terms). Derived metrics follow Eqs. (29)–(30) (Section 4.6). "NA" indicates data not available in the source; "-" indicates not applicable.

	Photovoltaic				PCM						Coupling	Study type
	Material	Power (W)	NOCT (°C)	Efficiency (%)	Organic / Inorganic /Eutectic	Phase-change temperature (°C)	Latent heat of fusion (kJ/kg)	Thermal conductivity in the liquid phase (W/(mK))	Thermal conductivity in the solid phase (W/(mK))	Thickness (mm)	(adhesive, glue, fastening, screwing)	Exp/Sim
[10]	Polycrystalline	65	NA	12.7	Eutectic (75.2% by weight of 98% pure capric acid and 24.8% by weight of 98% pure palmitic acid)	22.5	173	0.14	0.14	40	Gluing	Yes/No
					Inorganic (Salt hydrate Calcium chloride hexahydrate $CaCl_2{\cdot}6H_2O$)	29.8	191	0.56	1.08			
					Eutectic (75.2% by weight of 98% pure capric acid and 24.8% by weight of 98% pure palmitic acid)	22.5	173	0.14	0.14			
					Inorganic (Salt hydrate Calcium chloride hexahydrate $CaCl_2{\cdot}6H_2O$)	29.8	191	0.56	1.08			
[34]	Polycrystalline	40	NA	15	Organic (RT40)	38-43	134-156	0.2	0.2	34	Gluing	Yes/Yes
[55]	Monocrystalline	85	47	13.1	Organic (RT20)	21.23	140.3	0.2	0.2	30	Gluing	No/Yes
[56]	Polycrystalline	20	47	NA	Organic (RT44)	41-44	250	0.2	0.2	40	Screwing	Yes/No
[1]	Polycrystalline	50	45	12.35	Organic (RT35)	35	240	0.2	0.2	20	NA	No/Yes
[57]	Monocrystalline	100	NA	17.3	Organic (RT35)	29-36	160	0.2	0.2	25, 30	NA	No/Yes
[58]	Monocrystalline	50	45	15.6	Organic (Paraffin Wax)	5 to 60 (1 °C intervals)	210	0.15	0.24	50	NA	No/Yes
[59]	Monocrystalline	100	45	15.15	Organic (Paraffin Wax)	34.9-42	195.2	0.2	0.2	49	Screwing	Yes/No
[37]	Polycrystalline	30	NA	NA	Organic (White petroleum jelly PCM)	36-60	NA	0.18	0.18	20	Bolts	Yes/No
					Organic (White petroleum jelly PCM: 70% copper, 20% powder of graphite 10%)			92.1	92.1			
[60]	Monocrystalline	10	NA	NA	Organic (Paraffin 42-44)	42-72	195	0.22	0.22	20	NA	Yes/No
[61]	Polycrystalline	50	47	11.1	Organic (RT 25)	26.6	232	0.18	0.19	20	Gluing	No/Yes
[62]	Polycrystalline	50	47	11.1	Organic (RT 25)	26.6	232	0.18	0.19	20	Gluing	No/Yes
[63]	Polycrystalline	50	47	11.1	Organic (RT 25)	26.6	232	0.18	0.19	20	Gluing	No/Yes
[64]	Polycrystalline	65	NA	12.7	Eutectic (75.2% by weight of 98% pure capric acid and 24.8% by weight of 98% pure palmitic acid)	22.5	173	0.14	0.14	40	Gluing	Yes/Yes
					Inorganic (Salt hydrate $CaCl2{\cdot}6H_2O$)	29.8	191	0.56	1.08			
[65]	Polycrystalline	20	47	NA	Organic (RT42)	38-43	165	0.2	0.2	39	Screwing	Yes/No
[36]	Monocrystalline	250	45	15.54	Organic (RT28HC)	28	245	0.2	0.2	35	Adhesive	Yes/Yes
[66]	Monocrystalline	50	NA	15.5	Organic	30-32	200	0.2	0.2	19	Adhesive	Yes/No
[67]	Polycrystalline	40	NA	16.5	Organic (RT42)	38-43	165	0.2	0.2	10, 20, 30	NA	Yes/No
[68]	Thin Film	130	46	9.3	Organic (RT27)	25-28	184	0.76	0.88	45	NA	Yes/No
[69]	Polycrystalline	260	47	15.29	Inorganic (Hydrated Salt HS36)	36	167	0.47	0.5	30	Thermal paste and grease	Yes/No
[70]	Monocrystalline	50	45	15.8	Organic (RT42)	41.76	140	0.2	0.2	40	NA	Yes/No
[71]	Polycrystalline	100	45	14.5	Organic (OM35)	35-39	197	0.16	0.2	-	NA	Yes/Yes
[72]	Monocrystalline	305	48	18.6	Inorganic (InfiniteR18, InfiniteR29, PCM Bulk 48)	Experimental (18, 29, 48)	200	0.54	1.09	Experimental (6, 6, 11.11)	Thermal paste and aluminum bars	Yes/Yes
					Inorganic (InfiniteR)	30-60 (5 °C intervals)				5-30 (5 mm intervals)		
[73]	NA	NA	NA	NA	Organic (Paraffins RT28HC and OM29)	28, 29	250, 194	0.2, 0.293	0.2, 0.172	10-50	-	No/Yes

(continued on next page)

Table 2 (*continued*)

	Study location		Period			Analysis type						Results									
	Country, City	Köppen–Geiger climate class	Days	Starting date	Ending date	Parametric analysis	Ene	Eco	Env	Code	Model	E_{PV} (Wh)	$E_{PV\text{-}PCM}$ (Wh)	ΔE (%) (PEP)	η_{PV} (%)	$\eta_{PV\text{-}PCM}$ (%)	Δη (pp)	EEP (%)	$T_{p,PV}$ (°C)	$T_{p,PV\text{-}PCM}$ (°C)	ΔT (°C)
[10]	Ireland, Dublin	Cfb	1	12/09/2009	12/09/2009	-	Yes	Yes	-	-	-	33.4	35.7	6.89	10.0	10.7	0.70	7.00	49.0	43.0	6.0
	Ireland, Dublin	Cfb	1	12/09/2009	12/09/2009							33.4	36.5	9.28	10.0	11.0	1.00	10.00	49.0	40.0	9.0
	Pakistan, Vehari	BWh	1	30/10/2009	30/10/2009							43.0	45.8	6.51	13.1	13.9	0.80	6.11	63.0	51.0	12.0
	Pakistan, Vehari	BWh	1	30/10/2009	30/10/2009							43.0	47.5	10.47	13.1	14.5	1.40	10.69	63.0	42.0	21.0
[34]	UAE, Al Ain	BWh	365	01/01/2015	31/12/2015	-	Yes	Yes	-	-	Finite difference	27.8	32.5	16.60	15.0	20.9	5.90	39.33	72.0	62.0	10.0
																			53.0	44.4	8.6
[55]	Saudi Arabia, Dhahran	BWh	1	01/06/1990	01/06/1990	Yes (phase-change temperature)	Yes	-	-	-	Finite difference	-	-	-	13.1	18.1	5.00	38.17	-	-	-
[56]	Egypt, Benha	BWh	1	13/12/2020	13/12/2020	-	Yes	-	-	-	-	8.7	9.3	6.90	-	-	-	1.85	46.7	44.8	1.9
			1	12/01/2021	12/01/2021							8.2	8.7	6.10	-	-	-	3.38	48.6	45.0	3.6
			1	09/02/2021	09/02/2021							11.4	12.6	10.53	-	-	-	4.14	54.5	47.3	7.2
[1]	India, Allahabad	Cwa	31	01/05/2011	31/05/2011	Yes (tilt angle and wind speed)	Yes	-	-	COMSOL Multiphysics 5.0 software	FEM, CFD methods	-	-	5.00	-	-	-	5.00	60.0	54.9	5.1
[57]	-	-	-	-	-	Yes (ambient temperature and wind speed)	Yes	-	-	Matlab code and Ansys Fluent	Finite difference, CFD methods	-	-	-	15.5	17.3	1.80	11.61	-	-	-
[58]	USA, Agua Caliente	BWh	365	01/07/2012	30/06/2013	-	Yes	Yes	-	-	Finite difference	-	-	-	-	-	-	6.00	-	-	-
	India, Charanka	BSh	365									-	-	-	-	-	-	5.00	-	-	-
	China, Golmud	BWk	365									-	-	-	-	-	-	5.00	-	-	-
	Ghana, Nzema	Aw	365									-	-	-	-	-	-	6.00	-	-	-
	Germany, Neuhardenberg	Cfb	365									-	-	-	-	-	-	5.00	-	-	-
[59]	China, Shanghai	Cfa	2	18/07/2018	19/07/2018	-	Yes	-	-	-	-	20.5	21.6	5.17	-	-	-	5.18	68.7	53.0	15.7
[37]	Lebanon, Al-Khyara	Csa	1	16/05/2015	16/05/2015	-	Yes	-	-	-	-	-	-	-	-	-	-	3.00	66.3	65.6	0.7
	Lebanon, Al-Khyara	Csa	1	20/05/2015	20/05/2015							-	-	-	-	-	-	5.80	62.2	56.8	5.4
[60]	Laboratory conditions	Cfb	-	-	-	Yes (PCM materials)	-	Yes	-	-	-	-	-	-	-	-	-	4.60	-	-	-
[61]	-	-	-	-	-	Yes	Yes	-	-	Ansys Fluent	Finite volume	171.0	190.0	11.11	17.1	19.0	1.90	11.11	-	-	19.0
[62]	Spain, Madrid	Csa	-	-	-	-	Yes	-	-	Ansys Fluent	Finite volume	-	-	-	6.6	9.7	3.10	46.97	-	-	-
	Spain, Benidorm	BSh										-	-	-	8.4	11.6	3.20	38.10	-	-	-
[63]	-	-	-	-	-	Yes	Yes	-	-	Ansys Fluent	Finite volume	-	-	-	-	-	-	-	-	-	-
[64]	Ireland, Dublin	Cfb	1	12/09/2009	12/09/2009	-	Yes	-	-	-	-	41.6	41.7	0.34	-	-	-	1.00	49.0	43.0	6.0
	Pakistan, Vehari	BWh	1	30/10/2009	30/10/2009							31.9	33.4	4.41	-	-	-	4.40	63.0	46.0	17.0
	Ireland, Dublin	Cfb	1	12/09/2009	12/09/2009							41.6	42.3	1.76	-	-	-	1.80	49.0	39.0	10.0
	Pakistan, Vehari	BWh	1	30/10/2009	30/10/2009							31.9	34.4	7.67	-	-	-	7.70	63.0	42.0	21.0
[65]	Egypt, Benha	BWh	365	01/08/2020	31/07/2021	-	Yes	-	-	-	-	-	-	4.50	-	-	-	4.50	60.9	52.0	8.9
[36]	Slovenia, Ljubljana	Cfb/Cfa	7	14/10/2013	21/10/2013	-	Yes	-	-	Ansys Fluent	-	-	-	1.10	-	-	-	1.10	75.5	44.0	31.5
[66]	China, Hefei	Cfa	2	08/10/2017	09/10/2017	-	Yes	Yes	-	-	-	-	-	1.90	-	-	-	1.90	56.5	54.0	2.5
[67]	Egypt, Qena	BWh	95	20/06/2021	22/09/2021	Yes	Yes	-	-	-	-	-	-		-	-	-	14.4 (max)	-	-	-
[68]	Greece, Chania	Csa	365	01/07/2016	30/06/2017	Yes	Yes	Yes	Yes	-	-	-	-	9.40	-	-	-		-	-	26.1
[69]	India, Tamil Nadu	Aw	1	25/04/2022	25/04/2022	Yes	Yes	-	-	-	-	-	-	7.57	-	-	-	9.90	74.5	51.8	22.7
[70]	Iraq, Babylon	BWh	7	12/03/2023	19/03/2023	Yes	Yes	-	-	-	-	-	-	7.20	-	-	-	6.90	-	-	12.6
[71]	India, Guwahati	Cwa	1	-	-	Yes	Yes	-	-	Matlab	Artificial neural networks	54.5	65.9	20.95	11.2	12.5	1.39	12.47	-	-	-
[72]	Italy, Milan	Cfa	47	01/06/2024	17/06/2024	Yes (PCM materials)	Yes	Yes (Qualitative)	Yes (Qualitative)	-	-	3565.0	3542.0	-0.65	15.3	15.1	-0.14	-0.92	67.9	55.3	12.6
													3677.0	3.14		15.5	0.21	1.37		52.1	15.8
													3809.0	6.84		15.5	0.25	1.64		41.8	26.1
										Matlab	Lumped Parameter model	3565.0	(Optimal PCM melting 45 °C)	6.60	-	-	-	-	-	-	-
													(Optimal PCM thickness 10 mm)	6.90							
[73]	Mexico, Villahermosa	Am	365	Yearly		Yes (PCM materials)	Yes	-	-	-	Global Energy Balance and Effective Heat Capacity Method	-	0.18 and 0.16 (35 mm-RT28HC and OM29)	-	-	-	-	-	-	-	11.23 and 10.25 (PCM RT28HC and OM29)
	Mexico, Hermosillo	BSh											0.1 (35 mm-RT28HC and OM29)	-	-	-	-	-	-	-	6.44 and 6.81 (PCM RT28HC and OM29)

Notes: (i) When only η or E were reported, EEP/ΔE were computed directly from the source values; (ii) when only temperatures are reported, ΔT is computed from $T_{p,PV}$ and $T_{p,PV\text{-}PCM}$; (iii) units are standardized (°C, W/m^2, Wh); (iv) examples: [56] reports EEP = 1.85%, 3.38%, 4.14% with corresponding ΔT reductions of 1.9 °C, 3.2 °C and 7.2 °C across periods; [72] (Milan) shows ΔT ≈ from 12.6 to 26.1 °C and EEP ≈ from −0.92% to 1.64% across different PCM phase-change temperatures. Exp: experimental analysis; Sim: Simulation analysis; Ene: Energy analysis; Eco: Economic analysis; Env: Environmental analysis; NA: Not available

resulting in the development of several charts that illustrate various indicators pertinent to this research area. As depicted in Fig. 2, related only to the most relevant research available in the literature, the investigation of PV-PCM systems has gained momentum over the past decade, with an increasing interest in this technology. Notably, four significant articles were published in the two-year period 2024–2025, indicating a sustained upward trend in research activity in this field.

In this analysis, 45.83 % of the publications reviewed were exclusively experimental, while 33.33 % were solely theoretical, comprising numerical simulations validated against established data. The remaining 20.83 % encompassed both theoretical and experimental investigations of PV-PCM systems.

The literature indicates that approximately 83.33 % of the most pertinent articles relevant to this research were published in journals by Elsevier. Furthermore, 8.33 % of the studies appeared in journals published by MDPI, while the remaining 8.33 % included articles from other publishers, such as Springer.

The majority of studies on PV-PCM systems predominantly utilize polycrystalline (54.17 %) and monocrystalline (37.50 %) PV modules, with a limited number examining thin-film PV technology. The nominal power output of these PV systems typically ranges from 10 W to 305 W, with variations attributed to the type of PV material used.

Most studies report nominal operating cell temperatures (NOCT) between 45 °C and 48 °C for both monocrystalline and polycrystalline PV modules, while thin-film PV modules operate at 46 °C. The efficiency of the PV systems examined varies between 9.3 % and 18.6 %, with monocrystalline modules consistently achieving higher efficiencies up to 18.6 % compared to polycrystalline modules, which generally exhibit efficiencies in the range of 11.1 % to 16.5 %.

The analysis of the literature reveals a diverse array of PCMs utilized in the studies, including organic, inorganic, eutectic mixtures, and salt hydrates. The selection of a specific PCM for integration with PV systems is influenced by key characteristics such as melting point, latent heat, and thermal conductivity. An ideal PCM should possess attributes such as chemical stability, non-toxicity, non-corrosiveness, and cost-effectiveness, in addition to a large latent heat capacity and high thermal conductivity [24]. A PCM only delivers latent cooling when the PV back-surface temperature exceeds the phase-change temperature for a sufficient period during the day and then falls below it sufficiently at night to re-solidify. Hence, the phase-change temperature should be high enough to avoid premature melting in mild conditions, yet low enough to guarantee daily activation and full overnight reset.

Fig. 3 illustrates the distribution of various PCMs utilized in prior studies for the cooling of PV modules. Furthermore, Table 2 enumerates the PCMs referenced in the literature matrix for PV module cooling, detailing the significant characteristics of each material. Organic PCMs, such as RT type and paraffin wax, dominate the research landscape, likely due to their favorable phase-change temperatures and high latent heats of fusion for integration with PV systems. Inorganic PCMs, such as hydrate salts, are also studied, albeit less frequently. The predominance of organic PCMs (~70 %) reflects cost and ease of encapsulation but also biases reported performance and safety profiles; comparisons with salt hydrates/eutectics (~30 %) should account for organics' lower conductivity/flammability versus inorganics' subcooling/corrosion tendencies.

The phase-change temperatures of various PCMs utilized in PV systems range from 5 °C to 60 °C. The latent heat values of these PCMs span from 134 kJ/kg to 250 kJ/kg, while thermal conductivity values for PCMs, in both liquid and solid phases, are generally low, predominantly falling within the range of 0.14 W/(mK) to 1.09 W/(mK). These values indicate a need for enhancements in the thermal conductivity of PCMs, particularly in their solid state, to improve their overall effectiveness in PV-PCM systems. Notably, a study utilizing PCM with copper and graphite powders reports very high thermal conductivity values, reaching up to 92.1 W/(mK) [37].

To facilitate the phase change from solid to liquid and vice versa, PCMs are encapsulated to prevent material loss. Two primary encapsulation techniques are employed: macro-encapsulated PCMs and micro-encapsulated PCMs. PCM is referred to as macro-encapsulated when the size of the encapsulation exceeds 1 mm. In this type of macro-encapsulation, PCM is contained within tubes, pouches, rectangular plates, or spherical balls. When the encapsulation size ranges from 1 μm to 1000 μm, PCM is considered to be microencapsulated [71]. The majority of existing literature has concentrated on macro-encapsulated PCMs, with relatively few studies examining micro-encapsulated options, primarily due to the lower costs and greater volume capacity associated with macro-encapsulation. Most investigations utilize PCMs encapsulated within rectangular aluminum containers affixed to the rear of PV modules; however, alternative encapsulation methods, such as plastic or aluminum pouches, have also been explored. Organic PCMs are generally preferred due to their non-reactive nature with encapsulating materials and the infrequent occurrence of leakage issues, in contrast to inorganic PCMs, which are prone to such problems. Additionally, organic PCMs exhibit minimal subcooling, although their low thermal conductivity remains a significant challenge. Various heat transfer enhancement techniques have been investigated to address this limitation, as failing to do so may hinder the expected performance outcomes. Conversely, the corrosive properties and tendency for subcooling in inorganic compounds restrict their application in PV-PCM studies [71]. Inorganic PCMs may react with their encapsulating materials, resulting in leakage that can compromise PV module integrity and overall system performance. It is important to highlight that fatty acids and paraffin-based PCMs are highly flammable.

A variety of coupling methods are implemented across different studies, including gluing, screwing, thermal paste application, bolt connections, aluminum bars, and adhesive materials. Gluing and screwing are the most commonly employed methods, providing effective integration of PCMs with PV systems. Notably, about 30 % of studies utilize gluing as the primary coupling technique, likely attributed to its ease of application and the reliability of thermal contact. The choice of coupling materials, such as thermal paste, glue, adhesives, and metal bars, can significantly impact the thermal performance of PV-PCM systems due to the contact resistance; however, this aspect is often inadequately addressed in the literature.

Most studies adopt simulation-based approaches to predict the performance of PV-PCM systems, frequently employing finite difference, computational fluid dynamics (CFD), or finite volume methods. While experimental setups are also common, fewer studies combine experimental work with simulation support to validate results and conduct optimization analyses.

The experiments or simulations detailed in these publications were conducted across 25 different locations representing a range of climatic zones, classified according to the Köppen climate classification system. The location serves as a critical factor in the selection criteria for PCMs, as the maximum temperature that a PV module can achieve is contingent upon solar irradiation, which is inherently linked to the study location. Fig. 4 illustrates the specific locations and climatic zones in which researchers have explored the impact of PV-PCM systems on enhancing electrical power output and efficiency.

Research has been conducted in a variety of global locations across different climate zones, including:

- Tropical climates (e.g., Aw and Am) such as Mexico, India, and Ghana, characterized by stable high temperatures at sea level and low elevations.
- Arid (desert and semi-arid) climates (e.g., BWh, BSh, BWk) such as Pakistan, Egypt, UAE, Saudi Arabia, China, Spain, Iraq, Mexico, and India, where elevated temperatures may exacerbate PV heating.
- Temperate climates (e.g., Cfb, Cfa, Csa, Cwa), including Ireland, India, China, Lebanon, Germany, Spain, Greece, and Italy, where PCMs assist in stabilizing PV temperatures throughout varying seasonal conditions.

This geographical diversity underscores the adaptability of PCM technology to different climates while also revealing research gaps, particularly in regions experiencing extreme temperature variations or high humidity.

Because studies cluster in warm/arid zones, reported ΔT and efficiency gains likely represent upper-bound performance; maritime/colder climates remain under-sampled, limiting the generalizability of average benefits.

In temperate oceanic sites (Cfb), choosing a phase-change temperature around 30–42 °C typically gives moderate daytime activation with reliable overnight reset; pushing it higher risks under-activation on cool or windy days. In warm-summer/Mediterranean climates (Cfa/Csa), 35–50 °C generally delivers regular activation with acceptable reset outside heatwaves, whereas too low a phase-change temperature (below ~ 32 °C) tends to over-activate and dilute latent effectiveness. In arid or semi-arid locations (BWh/BSh), 45–60 °C aligns with sustained activation and the largest observed ΔT/EEP, but nightly reset can be incomplete at peak summer temperatures; cascaded layers (e.g., ~38 °C plus ~ 52 °C) or season-specific selections help mitigate this.

Practically, the phase-change temperature should be selected so that typical midday PV back-surface temperatures lie about 5–15 °C above it, while night-time minima fall at least 5–10 °C below it in the target season. In hot/arid sites, cascaded PCMs or a slightly higher phase-change temperature should be considered to preserve nightly reset. For year-round operation, the phase-change temperature should be matched to the intended season of benefit (summer peak versus shoulder months) and stated explicitly. When only ambient data are available, activation can be judged using the study's reported PV temperatures in Table 2 as proxies.

Many studies have demonstrated enhanced energy yield through PCM integration, with efficiency improvements typically ranging from + 1 % to a maximum of + 14.4 % in specific instances. In some cases, reductions in PV module operating temperature have almost reached 30 °C [36,72], contributing to more stable and efficient performance.

Using the performance indicators defined in Section 4.6, we derived study-level metrics where source data permitted, as shown in Fig. 5. Across experiments that reported both baseline and PV-PCM values, ΔT commonly falls in the 10–30 °C range, with multiple studies reporting values near the upper end under hot/arid conditions (e.g., Italy–Milan scenarios and arid-zone sites). Corresponding electrical improvements span from modest (≈+1–3 %) to double-digit gains in specific instances (e.g., +1.85 to + 4.14 % in Egypt [56]; scenario-dependent + 1.37 to + 1.63 % in Milan [72]). These results confirm the sensitivity of gains to climate and PCM melting range. The full per-study ΔT, Δη/EEP, and ΔE/PEP values are reported in Table 2, enabling side-by-side comparison of materials, climates, and integration methods.

Overall, this analysis highlights the significant influence of climatic conditions and phase-change temperatures on the benefits associated with increased electrical energy production and enhanced electrical efficiency.

To enrich the literature review, a global scientometric review was developed by using the Scopus database. The study of PV-PCM is recent, and there is a need to investigate the current research status, as well as an understanding of how this field has developed over time, especially in the recent decade. The scientometric study attempted to review the PV-PCM system research published so far to provide researchers with complete and insightful knowledge maps to assist the author's review analysis. In this work, a search was made to identify various academic publications concerning the topic of hybrid systems, with the last update taking place on May 20, 2025. Scopus database was used, and all document types were selected: article, review, book, book chapter, conference paper, and data paper, both with and without open access. The search results were refined to include only documents written in the English language. The overall query used to rebuild the development history of the use of PCM-cooled PV systems is (photovoltaic AND phase AND change AND material AND cooling). The time span of literature retrieval was set from "All Years" to "Present". The study recruited a total of 801 published PV-PCM articles, of which 531 were original research articles, 130 were conference proceedings, and 96 were paper reviews. Fig. 6 illustrates the percentage of documents by type. The record set is dominated by journal articles, with relatively few reviews and proceedings; this imbalance limits formal synthesis and may contribute to heterogeneity in reported gains and methods across studies.

Fig. 7 shows how the distribution of the 801 bibliographic records on the research topic under review varies each year in the period 2006–2025. The first paper, published by Jiajitsawat and Duffy and presented at two different conferences in 2006, aimed to design and validate a portable solar refrigeration system integrating direct-coupled PV thermoelectric modules (TEMs) with latent heat energy storage using water as the PCM [74,75]. The system was intended to maintain vaccine temperatures between 2 and 8 °C for at least four days without access to grid electricity. The objectives included both theoretical validation through modeling and experimental testing, including a field feasibility study in remote Peruvian villages lacking electrification and with high numbers of unvaccinated children.

The analysis showed that publications concerning PV-PCM systems have significantly increased from 2018 to 2025, showing a remarkable development in the last ten years. Before 2014, only some isolated research had been developed. This is justifiable because, during these years, the PV-PCM concept was still at a very early stage. In the year 2014, a relatively significant number (17) was recorded for the first time, and the trend started to increase continuously. This may be due, in addition to the greater interest of researchers in this area, also to the greater concern and attention towards the environment and climate change, the need to seek new energy sources and storage systems, and the interest of governments in encouraging the use of these types of technologies, and enacting ad-hoc Directives. Note that the study considers, for the year 2025, publications in the first 5 months of the year. As highlighted in Fig. 8, the most productive countries in this research field are India and China, followed by Malaysia and Saudi Arabia. Among the European Countries, only France and Italy provided a significant effort on this topic.

The concentration of outputs in India and China indicates a bias toward hot/high-irradiance contexts and local standards; evidence from cooler European/North American settings is comparatively sparse,

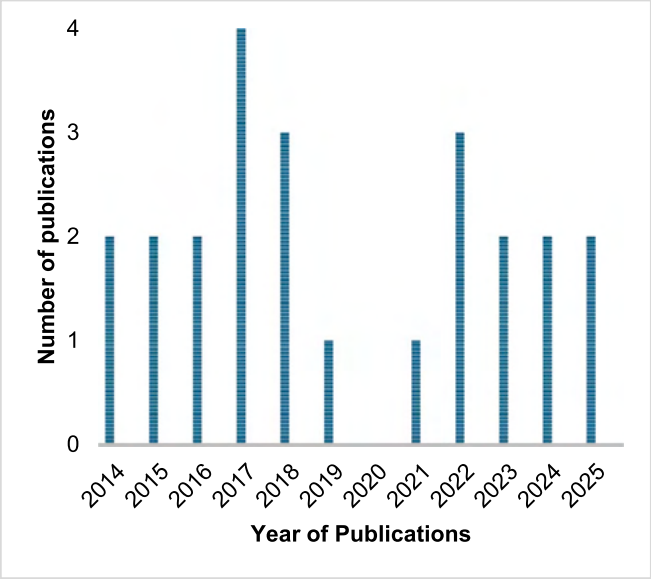

Fig. 2. Trend of the selected most relevant papers in the past ten years.

which may affect the transferability of design recommendations.

4. PV-PCM models

This section provides an in-depth analysis of the publications related to PV modules integrated with PCMs, detailing the models employed in these studies and elucidating the primary equations associated with them. To effectively characterize the thermal and electrical phenomena that occur within PV modules integrated with PCMs, researchers have developed a diverse range of mathematical models over time, which exhibit varying degrees of complexity. These models are crucial for comprehending the interactions between the PV module and the PCM, as they facilitate the simulation of heat transfer dynamics and electrical energy conversion under various operating conditions.

Among the more sophisticated modeling approaches, enthalpy- or effective heat capacity-based methods coupled with finite difference methods are frequently employed to provide detailed descriptions of thermal processes. The enthalpy model specifically emphasizes the role of latent heat during phase transitions of the PCM, integrating energy release and absorption into the thermal balance equations. As illustrated in the research by Y. Kozak and G. Ziskind, enthalpy models effectively capture the behavior of materials undergoing phase changes from solid to liquid and vice versa [76]. This model excels in addressing complex scenarios involving melting and solidification, particularly in situations where the thermal inertia of the solid mass cannot be overlooked. Conversely, finite difference models address heat transfer equations through spatial and temporal discretization techniques, thereby offering a comprehensive representation of the temperature distribution within the PV module, as highlighted in the work of Lo Brano et al. [77]. While these methods provide high accuracy, they necessitate substantial computational resources and typically require the separate modeling of thermal and electrical phenomena. Considering that thermal and electrical models are governed by distinct physical principles, it becomes essential to couple the thermal models with an electrical model that accurately depicts the behavior of the PV module. Among the various electrical modeling approaches, the five-parameter model is one of the most widely adopted and precise solutions available. This model provides an accurate representation of the current–voltage (I-V) characteristics of the module, incorporating critical factors such as internal resistance, saturation current, and the impact of temperature on electrical performance. The five-parameter model is particularly esteemed for its capability to accurately reflect the electrical behavior of the module under actual operating conditions, making it an invaluable tool when integrated with complex thermal models.

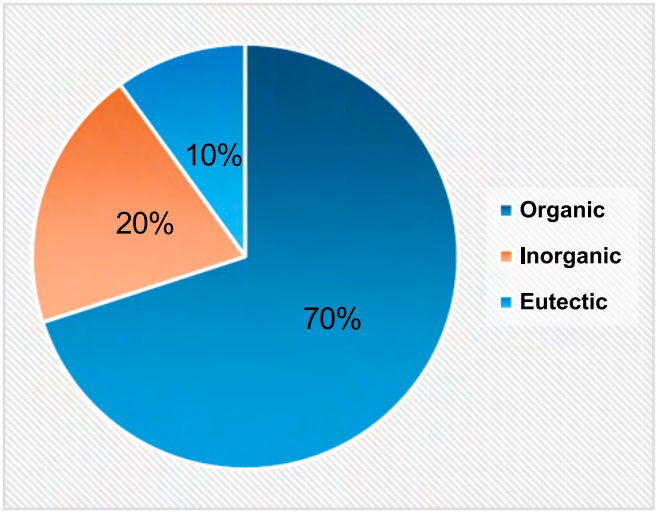

Fig. 3. Type of PCM used in PV-PCM systems.

To compute and thermally analyze the PCM module, several fundamental assumptions are commonly established [55]:

- Heat transfer within the PCM occurs solely via conduction.
- The thermophysical properties of the PCM remain constant and uniform in both phases.
- The melted PCM is Newtonian and incompressible.
- The PCM is considered homogeneous and isotropic.

Additional assumptions utilized in the analysis include [1,61]:

- Heat losses from the PV side surfaces are negligible.
- The incident solar radiation is uniformly distributed across the surface of the PV module.
- Contact resistances within the PV cell are disregarded.
- No dust or other agents are deposited on the module's surface that affect the module's absorptivity.
- The flow due to the melting of PCM is laminar, and the radiation and three-dimensional convection effects of melted PCM are negligible.

4.1. PV-PCM thermal models

Fig. 9 shows a typical configuration of a PV-PCM system as described in Ref. [59].

When the PV panel absorbs solar radiation, the portion not converted into electrical energy mostly turns into heat. As the temperature of the PV-PCM module rises, it releases heat to the surroundings via convective and radiative transfer at its surface. The thermal balance of a PV-PCM module was formulated by Al Najjar et al. on the basis of an electrical equivalent circuit schematizing all convective and radiative heat exchanges between the front and rear surfaces and the outdoor environment, as schematized in Fig. 10 [57].

This network consists of seven nodes with temperatures that are not yet determined. Each node's temperature is assumed to represent the average temperature across its cross-sectional area. In this thermal network, the PCM layer is divided into two parts: melted part and the solidification phase. Each is considered to have its own overall heat transfer coefficient, accounting for both conduction and convection.

4.1.1. PCM enthalpy model

An advanced model for analyzing the behavior of materials undergoing phase change is founded on the integration of the finite difference method with the enthalpy method [78,79]. Enthalpy-based methods, along with similar techniques that account for the release or absorption of latent heat, have been successfully employed in recent years to address phase change problems characterized by the movement of solid/liquid interfaces resulting from the heating or cooling of the investigated system. These methodologies were initially developed by Voller and Prakash [78] and Bennon and Incropera [79], and they have been significantly refined over time to accommodate a diverse range of systems and conditions.

The energy conversion of material undergoing a phase change can be expressed as Eq. (1) [55]:

$$\rho_{PCM}\frac{\partial H}{\partial t} = \nabla\cdot(k_{PCM}\nabla T) \tag{1}$$

This equation can be discretized with a full implicit discretization method to obtain a formulation that is independent of space and time step selection. Enthalpy methods incorporate latent heat into energy equations by assigning a nodal latent heat value to each computational cell based on its temperature. During the phase change, the nodal latent heat content of the cell is adjusted to reflect the release or absorption of

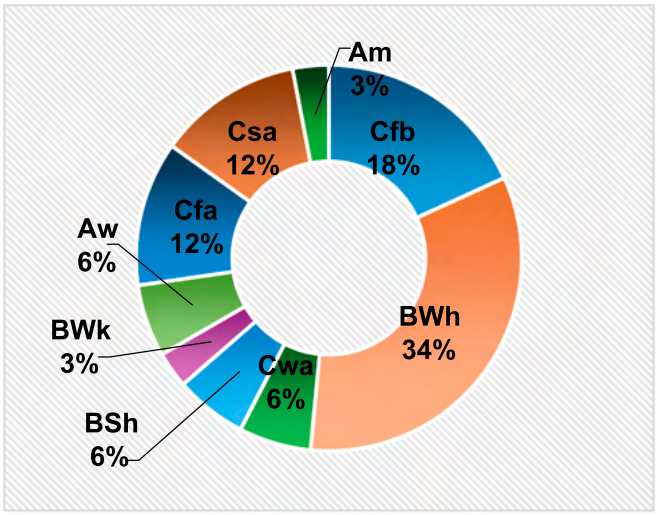

Fig. 4. Study location based on the Köppen–Geiger climate zones.

latent heat, which is represented in the energy equation as a source or sink term. A notable advantage of this approach is that it eliminates the necessity to explicitly consider the energy conservation conditions at the solid/liquid interface. The integration of latent heat during phase transitions is accomplished through the following enthalpy definition for each phase:

$$H = C_p T + \Delta H \tag{2}$$

where

$$\Delta H = \phi L_m \tag{3}$$

In these equations, C_p is the specific heat capacity, L_m is the latent heat, and ϕ is the liquid fraction, defined as:

$$\phi(T) = \begin{cases} 0 & for\ T < T_{sol} \\ \dfrac{T - T_{sol}}{T_{liq} - T_{sol}} & for\ T_{sol} < T < T_{liq} \\ 1 & for\ T > T_{liq} \end{cases} \tag{4}$$

Where $T_{sol} = T_m - \Delta T_m$ and $T_{liq} = T_m + \Delta T_m$, with $2\Delta T_m$ representing the temperature range over which phase change occurs. In this context, T_{liq} is the liquid temperature at which solid formation initiates, while T_{sol} is the temperature at which complete solidification occurs. This extended temperature range for solidification accounts for the physical scenario in which solid formation takes place as a permeable crystalline matrix coexisting with the liquid phase, often referred to as the mushy zone. Numerically, a linear approximation for the liquid fraction is required, as a step change could induce significant numerical instability. During the solidification of the PCM, latent energy is released at the interfaces separating the phases within the mushy region. Consequently, the total enthalpy of the system can be expressed as the sum of the sensible enthalpy H_S and the latent enthalpy H_l. These contributions are evaluated based on the following considerations:

$$H_s = \int_{T_{ref}}^{T} C_p dT \tag{5}$$

$$H_l = \phi L_m \tag{6}$$

The model described above facilitates the determination of the material's physical state and, consequently, its energy level based on the material temperature T.

Classical enthalpy–porosity treats the mushy region as a porous medium; results can be sensitive to the mushy-zone parameter and "effective viscosity" used to immobilize solids, sometimes causing numerical stiffness or unphysical "fluid-like" solid motion [76]. Advanced enthalpy formulations for close-contact melting address these issues by coupling force balance and melt flow without arbitrary constants. We therefore reserve CFD-grade enthalpy models for cases where melt convection/3D effects govern performance.

4.1.2. PCM effective specific heat method

Another advanced model for analyzing the behavior of materials undergoing phase change is founded on the integration of the finite difference method with the effective specific heat method [80]. The effective specific heat method formulation assumes conduction-dominated heat transfer through the PCM; it does not resolve natural convection in the liquid phase and requires choosing a finite phase change interval ΔT around the phase-change temperature T_m. This is appropriate for slender, encapsulated, or high-viscosity PCMs where buoyancy is suppressed and 1D through-thickness gradients dominate; validated PV-PCM studies justify this assumption and show agreement with experiments [61,77].

In this case, the heat conduction equation to be considered is:

$$\frac{\partial}{\partial x_i}\left(k(T)\frac{\partial T}{\partial x_i}\right) = \rho c_A \frac{\partial T}{\partial t} \tag{7}$$

where k(T) is the thermal conductivity, T is the temperature, ρ is the density, and c_A is the effective heat capacity. This approach employs the effective specific heat capacity c_A to manage latent heat during the phase change process. The effective specific heat approximates the phase change over a defined temperature range and typically represents the phase-change temperature [80]. The effective specific heat is defined by integrating the energy balance over this specified temperature range:

$$\int_{T_m - \Delta T}^{T_m + \Delta T} c_A dT = \int_{T_m - \Delta T}^{T_m} c_s dT + \Delta h + \int_{T_m}^{T_m + \Delta T} c_l dT \tag{8}$$

where Δh is the latent heat of fusion, c_s is the specific heat capacity in the solid state, and c_l is the specific heat capacity in the liquid state.

The effective specific heat capacity c_A can then be expressed as:

$$c_A = \begin{cases} c_s & for\ T < T_m - \Delta T \\ \dfrac{\Delta h}{\Delta T} + \dfrac{c_s + c_l}{2} & for\ T_m - \Delta T < T < T_m + \Delta T \\ c_l & for\ T > T_m + \Delta T \end{cases} \tag{9}$$

To avoid discontinuities at the phase change interface, a continuous sigmoid function can be used when ΔT is small:

$$c_A = c_s + (c_l - c_s)\frac{1}{1 + e^{-\alpha(T - T_m)}} + \frac{\alpha \Delta h}{e^{-\alpha(T - T_m)} + e^{\alpha(T - T_m)} + 2} \tag{10}$$

where α is a parameter that controls the smoothness of the transition.

4.2. PV-PCM electrical model

According to the thermal models described in Section 4.1, these systems offer a high degree of accuracy in the thermal analysis of the integrated module. However, for comprehensive characterization, it is essential to couple these thermal models with an electrical model. To assess the effective electrical energy output from the PV system and determine the overall module efficiency, a 4-, 5-, or 6-parameter electrical model can be utilized, as these models are capable of providing precise solutions. Furthermore, the PV efficiency, denoted as η_{PV}, must be calculated as a function of the maximum power generated by the PV module at any given time. The output power of the PV module is determined as:

$$P_{PV} = V_{PV} \cdot I_{PV} \tag{11}$$

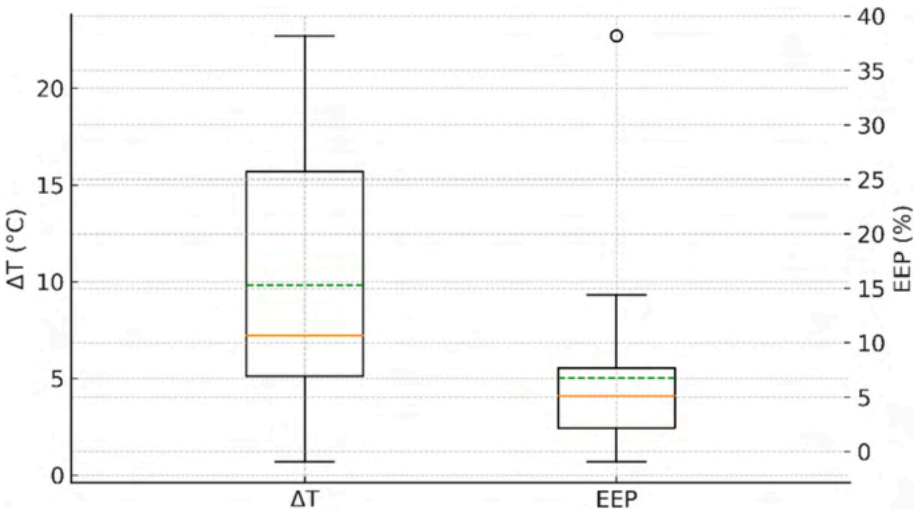

Fig. 5. Dual-axis boxplot of study-level performance derived from Table 2. Left axis: ΔT (°C) (PV back-surface temperature drop). Right axis: EEP (%) (enhancement in electrical efficiency).

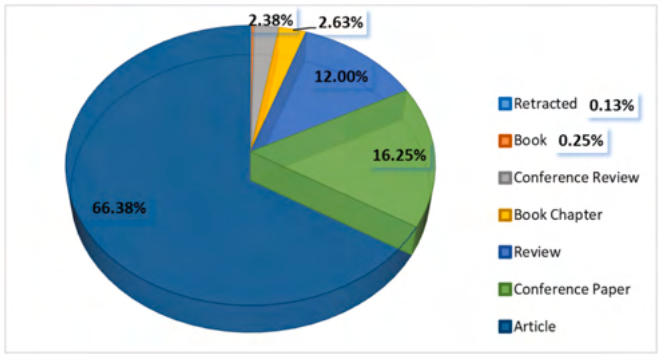

Fig. 6. Publication type distribution (period 2006–2025).

where I_{PV} and V_{PV} are the current and voltage output of the PV module, respectively.

As an example, in the case of the 5-parameter model [57], the unknown parameters are the light current I_L, diode reverse current I_0, series resistance R_s, shunt resistance R_{sh}, and modified ideality factor a. A graphical representation consistent with the considered model is shown in Fig. 11.

The maximum PV power and the corresponding efficiency are determined through the following three steps:

- Solving the five-parameter model, wherein the five parameters of the model are numerically derived under standard test conditions (STC) at $G_{ref} = 1000$ W/m^2 and $T_{c,ref} = 25$ °C.
- Calculating the parameters under actual operating conditions; the parameters established in the first step are adjusted to reflect the specific operating conditions corresponding to a given solar irradiance G and cell temperature T_c.
- Computation of the maximum power and the PV electrical efficiency η_{el} using the parameters calculated under the defined operating conditions:

$$P_{mp} = P_{PV}|_{mp} \tag{12}$$

$$\eta_{el} = \frac{P_{mp}}{A_{PV}G} \tag{13}$$

The overall efficiency η_{ov} of the PV/PCM system is expressed as the summation of the contributions from the PV module and the thermal efficiency η_{th} of the PCM:

$$\eta_{ov} = \eta_{el} + \eta_{th} \tag{14}$$

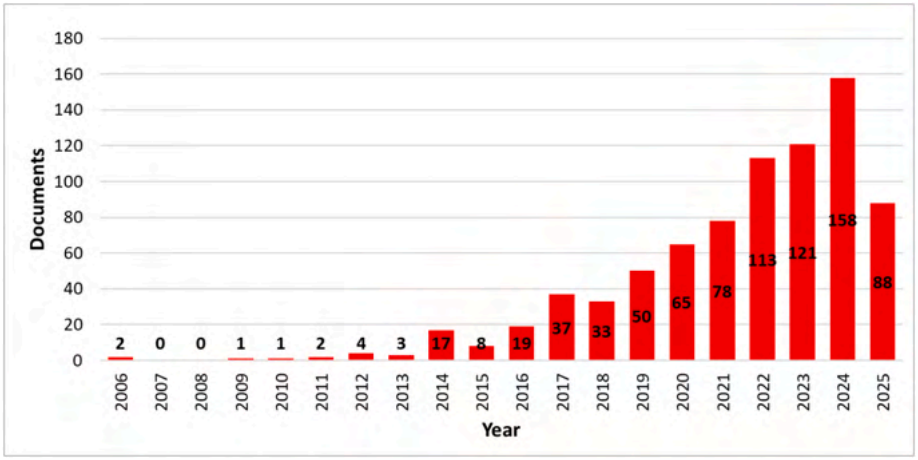

Fig. 7. Historical trend of published studies in PV-PCM systems (period 2006–2025).

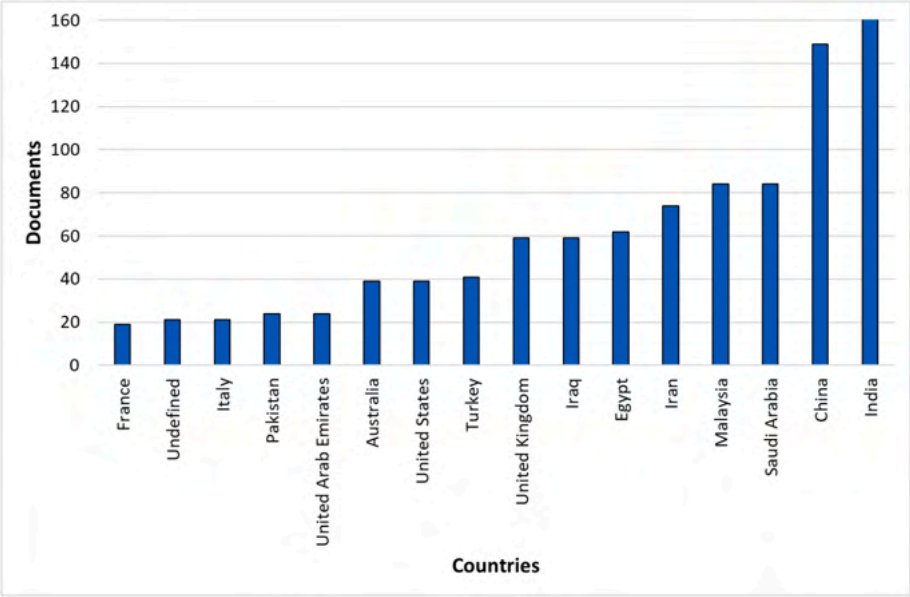

Fig. 8. Most productive countries in the PV-PCM research field (period 2006–2025).

4.3. PV-PCM simplified models

A simplified model for calculating indicators related to PV-PCM systems, such as efficiency, treats the system as a thermal system utilizing latent heat storage [35]. In this context, the energy balance for a PV system is governed by Eq. (15):

$$Q_{solar} = Q_{elec} + Q_{lost} + Q_{stored} \quad (15)$$

In this context, Q_{solar}, Q_{elec}, Q_{stored}, and Q_{lost} represent, respectively, the solar energy incident on the PV panel, the electrical energy output from the panel, the thermal energy stored within the panel, and the thermal energy lost from the module.

In the absence and in the presence of PCM, each term can be calculated by Eqs. (16)-(21):

$$Q_{solar} = GA_{PV}\Delta t \quad (16)$$

Here, G represents the intensity of global solar radiation striking the panel, A_{PV} is the panel's surface area, and Δt refers to the duration of the experiment. The value of Q_{elec} is specified by Eq. (17).

$$Q_{elec} = V_{oc}I_{sc}FF\Delta t \quad (17)$$

In this context, V_{oc}, I_{sc}, and FF refer to the open-circuit voltage, short-circuit current, and fill factor of the module, respectively.

$$Q_{lost-PV} = GA_{PV}(1-\alpha\tau) + h_{ca}A_{PV}(T_{PV} - T_{amb})\Delta t \quad (18)$$

In this context, τ represents the portion of solar radiation that passes through the top cover of the PV panel, while α indicates the portion of solar radiation absorbed by the cover. Tamb and T_{PV} refer to the ambient temperature and the surface temperature of the PV panel, respectively. Additionally, h_{ca} is the coefficient for combined convective and radiative heat loss from the PV panel. The heat lost by the PV-PCM is calculated using Eq. (19).

$$Q_{lost-PV-PCM} = GA_{PV-PCM}(1-\alpha\tau) + h_{ca}A_{PV-PCM}(T_{PV-PCM} - T_{amb})\Delta t \quad (19)$$

where $T_{PV\text{-}PCM}$ and $A_{PV\text{-}PCM}$ refer to the surface temperature and surface area of the PV-PCM system, respectively.

$$Q_{stored-PV} = C_{PV}\Delta T \quad (20)$$

$$Q_{stored-PV-PCM} = C_{PV}\Delta T + V_{PCM}\lambda\rho \quad (21)$$

For the sake of simplicity, it is usually assumed that a uniform temperature is maintained throughout the six layers of the module [55,72]. The heat capacity of the module is calculated using Eq. (22):

$$C_{PV} = \sum_{i=1}^{6} Ad_i\rho_i C_i \quad (22)$$

Q_{stored} is due only to the PCM sensible contribution, a function of area, thickness, density, heat capacity, and temperature difference, for the PV system, while for the PV-PCM system also the latent contribution also intervenes, dependent on PCM volume and density and latent heat of fusion.

The primary physical principle underpinning this simplified model is that the integration of PCM behind the PV module facilitates the storage of thermal energy that would otherwise be dissipated. This process of heat absorption effectively regulates the temperature of the PV module, resulting in an increase in its electrical output. Additionally, the thermal energy stored in the PCM represents an alternative energy source, which is of lower quality compared to electrical energy; therefore, a conversion efficiency of 30 % must be factored into this energy contribution. Eqs.

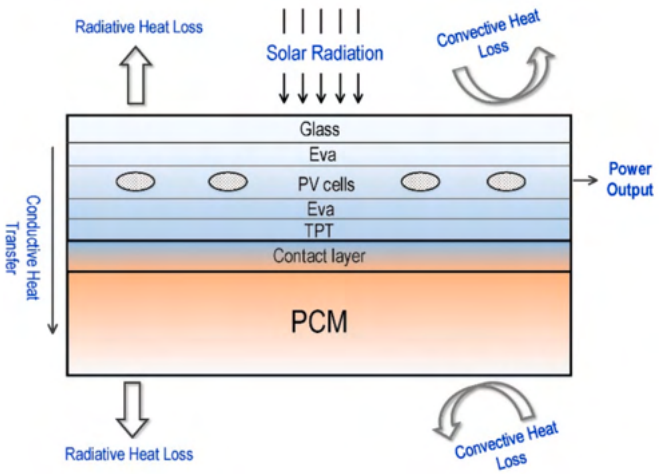

Fig. 9. Configuration of a typical PV-PCM system and the energy flow path [59].

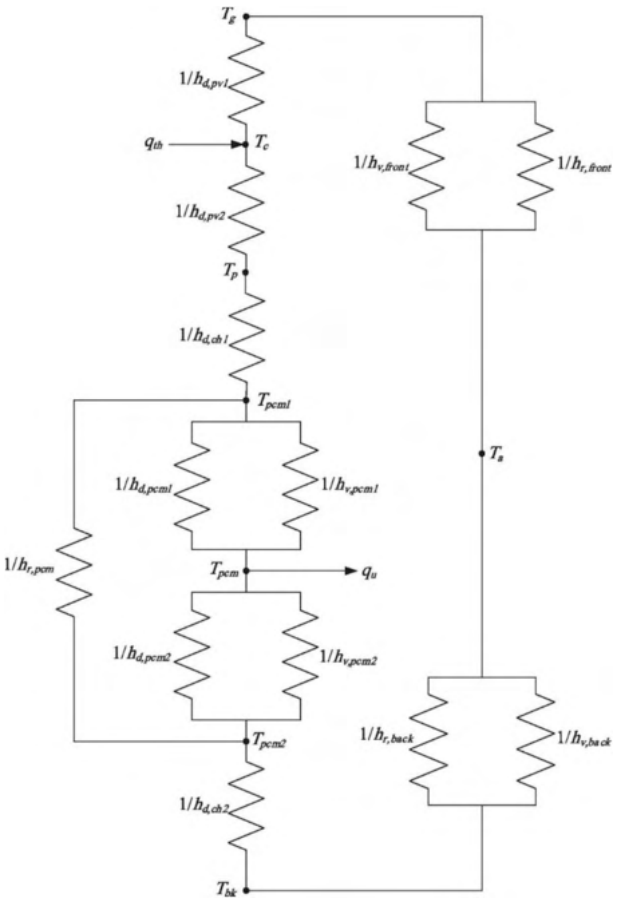

Fig. 10. Thermal network for the typical PV/PCM system [57].

(13) and (23) delineate the electrical energy efficiency and the thermal energy efficiency, respectively [35].

$$\eta_{th} = \frac{0.3Q_{stored}}{GA_{PV}} \tag{23}$$

Given that the quality of thermal energy differs from that of electrical energy, a conversion efficiency of 30 % is applied to transform thermal energy into equivalent electrical energy. The term Qsaved represents the additional savings in both electrical and thermal energy achieved by incorporating PCM into the PV system compared to the reference PV. These savings are calculated to assess the effectiveness of the PV-PCM systems in different climates, as outlined in Eq. (24).

$$Q_{saved} = (Q_{elec-PV-PCM} - Q_{elec-PV}) + 0.3(Q_{stored-PV-PCM} - Q_{stored-PV}) \tag{24}$$

This model represents one of the foundational approaches for estimating the energy savings and effectiveness of PV-PCM systems. To enhance the accuracy of these formulations, it is essential to incorporate heat transfer methodologies to elucidate and calculate specific terms more precisely.

Kibria et al. proposed a straightforward model that encompasses the three primary mechanisms of heat transfer [55]. In this framework, a portion of the incident solar radiation is transformed into electrical energy, while the remainder is converted into thermal energy. Subsequently, a fraction of this thermal energy is dissipated to the environment through convective and radiative losses. This led to the development of Eq. (25), which was then discretized using finite difference methods, resulting in Eq. (26) [55]:

$$q_{PV} = q_{solar} + q_{sky} - q_{convection} - q_{PCM} \tag{25}$$

$$T_{PV,t} = \left(\frac{q_{solar} + q_{sky} - q_{convection} - q_{PCM}}{C_{PV}}\right)\Delta t + T_{PV,t-1} \tag{26}$$

Eq. (26) provides the temperature at the successive instant as a function of the temperature at the previous instant, the time step, and the net heat transferred into the PV module.

As regards the electrical simplified models, one approach is characterized by the use of linear relations to calculate the electrical power and efficiency [70] in the form of:

$$\eta = \eta_{ref}\left[1 - \beta_{ref}\left(T_{PV} - T_{ref}\right)\right] \tag{27}$$

Here, β_{ref} is primarily a material property. The equation above represents the conventional linear expression for PV electrical efficiency, with the values of η_{ref} and β_{ref} provided by the PV manufacturer. Therefore, the total power output of the panel is given by:

$$P = \eta_{ref}[1 - \beta_{ref}(T_{PV} - T_{ref})]AG \tag{28}$$

4.4. Model choice: limits, computational cost, appropriate use cases

PV-PCM simulations span three practical families. Table 3 summarizes what each captures, where it breaks, and when to use it.

(A) Enthalpy–porosity CFD (2D/3D) [61]: solves continuity–momentum–energy and is required when natural convection in the melt, non-1D heat leaks (e.g., side-walls), or geometric features (fins/foams, micro-encapsulation distribution) control performance. Typical PV-PCM CFD assumes adiabatic side walls (2D); 3D models relax this and better represent realistic losses. These works show that melt convection measurably alters PV temperature and efficiency, especially for thicker PCM layers, tilt, and wind coupling.

Limitations [76]: (i) high computational cost; (ii) sensitivity to the mushy-zone parameter and effective-viscosity tricks used to "freeze"/"unfreeze" cells; (iii) potential numerical stiffness and even non-rigid "fluid-like" solid motion if parameters are poorly set, as highlighted in close-contact melting literature; advanced enthalpy formulations mitigate some of these issues.

When to use [61]: geometry optimization (fins, foams), thick PCM, strong buoyancy (high Rayleigh number), non-uniform heating, or when side-wall losses/3D effects are non-negligible.

(B) Effective specific-heat/1D finite-difference (EHC/FDM) [61,77]: treats latent heat as an elevated cA(T) across a small ΔT in Eq. (8), solving 1D conduction across layers. Multiple validated PV-PCM studies justify the 1D assumption where layer slenderness, encapsulation, or high melt viscosity suppress natural convection, and show good agreement with outdoor data.

Limitations [77]: (i) does not resolve melt convection; (ii) results depend on the chosen phase change interval ΔT; (iii) cannot evaluate lateral/edge losses or fins.

When to use [77]: thin/slender PCM layers, bagged/MEPCM configurations, BIPV back-layers, early design comparisons where conduction dominates and gradients are mainly through-thickness.

(C) Lumped/thermal-network (PV/T-PCM) [57]: replaces the PCM block with overall thermal conductance U correlations for solid/mushy/liquid phases in a PV/T network coupled to a five-parameter PV model. These models have been CFD- and experimentally validated, and are ~ 10^3–10^4 × faster (e.g., ~14 s vs ~ 16 h CFD for a multi-hour transient), enabling parametric scans and design charts (melting interval vs thickness, efficiency vs wind, tilt).

Limitations [57]: (i) no internal fields or interface tracking; (ii) requires calibration/choice of U across phases; (iii) not suited to shape optimization.

When to use [57]: techno-economic studies, controller co-design, climate/tilt/wind sweeps, and rapid screening of PCM thickness/phase-change temperature before refining with (A) or (B).

Practical guidance [61,77]: if melt convection is likely (thick PCM,

high tilt, warm ambient), step up from (B) to (A); if encapsulation suppresses convection or the target is system-level trade-offs, (B) or (C) are sufficient. Notably, many tilted PV-PCM studies include convective effects explicitly and document the influence of wind and side walls; others justify 1D when bags/viscosity stifle buoyancy.

In practice, model selection should reflect expected buoyancy (tilt/thickness/ambient), lateral losses, and study objective: use EHC/1D for conduction-dominated back layers, lumped networks for rapid design charts and control/TEA, and CFD enthalpy–porosity when convection and geometry set performance; these choices are broadly consistent with prior tilted and 3D PV-PCM analyses and recent fast, validated PV/T-PCM network models [57,61].

4.5. Model validation: verification, calibration, and external validation

Model credibility was strengthened by distinguishing verification (solving the equations right), calibration (parameter estimation from data), and validation (predictive accuracy against measurements not used for tuning). For enthalpy/porosity CFD, mesh and time-step independence should be demonstrated and the solver verified against canonical phase change benchmarks (e.g., square-cavity melting with multi-cellular natural convection), reporting liquid-fraction vs time and front morphology; typical independent solutions use O(200 × 200) grids with sub-millisecond time steps for 2-D cavities. Where possible, comparisons to well-characterized melting experiments (e.g., isothermal rectangular enclosures) should be provided, noting known discrepancies due to 3-D effects or boundary-condition imperfections. For effective specific-heat (EHC) conduction models, verification against analytical/semianalytical Stefan-type solutions is recommended for 1-D transients; validation should then proceed against a higher-fidelity enthalpy simulation for the same geometry to map the bias introduced by neglecting convection [77]. For lumped/thermal-network models, calibration should use independently measured thermo-optical inputs (e.g., DSC-derived latent heat and melting range; layer conductivities and heat capacities), followed by two-stage validation: (i) numerical cross-validation against CFD for internal state trajectories (cell temperature, PCM layer temperatures) and (ii) experimental validation under controlled indoor or outdoor conditions with matched boundary conditions. Report NRMSE(%), MAE, R^2 (or correlation r) for temperature time series and power, together with energy-balance closure and computation time.

As regards the experimental validation practices, module-level validation should instrument front glass, cell/backsheet, and at least two PCM depths; log plane-of-array irradiance, ambient temperature, wind speed, tilt/azimuth, and view-factor-consistent radiative surroundings. Indoor solar-simulator tests aid repeatability; outdoor tests establish robustness across diurnal transients [72]. Exemplary setups with extensive node instrumentation and boundary-condition control for PV-PCM modules are available in the literature and were used to validate model predictions [57]. Outdoor validations across climates further demonstrate generality [35]. Models should separate calibration and validation datasets (e.g., different days), disclose mesh/time-step tests (CFD), provide DSC/property sources for PCM (latent heat and melting interval used in the model), and publish error metrics (RMSE/NRMSE, MAE, R^2 or r, optional NSE), plus a brief runtime comparison to indicate fitness for parametric/design use [57].

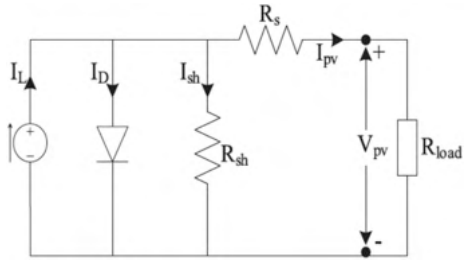

Fig. 11. Equivalent electrical circuit of the five-parameter model [57].

4.6. Performance indicators for PV-PCM systems

Indicators used to evaluate the PV-PCM performance improvement are the power enhancement percentage (PEP) and the enhancement in electrical efficiency (EEP) [70]:

$$PEP = 100\frac{P_{PV-PCM} - P_{PV}}{P_{PV}} \tag{29}$$

$$EEP = 100\frac{\eta_{PV-PCM} - \eta_{PV}}{\eta_{PV}} \tag{30}$$

The PEP can also be calculated in terms of energy. Also the temperature drop on the back and front surfaces of the module is a commonly used indicator to quantify the PCM passive cooling performance. These indicators were also used to compute the study-level values added to Table 2 (see Section 3).

5. Fire risks, cycling stability, and degradation in PV–PCM systems

5.1. Fire risks

Previous studies have reported PV temperatures reaching 75 °C during peak sunlight hours [36], particularly in arid conditions, thus necessitating caution in employing organic PCMs under such circumstances; inorganic materials are recommended as safer alternatives. Literature shows some practical strategies to mitigate fire risks for organic PCMs integrated in PV systems:

i. Material-level mitigations [81] (such as non-combustible surface barriers (e.g., aluminum foil / rigid films) to prevent wicking and surface flame spread or sequential impregnation (PCM followed by an insoluble liquid flame retardant), imparting self-extinguishing behavior;
ii. Encapsulation and shape-stabilized composites (e.g., paraffin supported in expanded graphite (EG), carbons, silica/clays, or polymer matrices) curb leakage and reduce effective fuel availability while improving thermal stability and conductivity, particularly valuable when PV back-surface temperatures approach ~ 70–75 °C [81,82].
iii. PV-specific integration guidance (hot, arid sites up to ~ 75 °C) [81–83]:
   a) Place PCM in metal cassettes/channels acting as heat spreaders and non-combustible barriers; maintain standoff from junction boxes, connectors, and cable trays.
   b) Route DC cabling outside PCM volumes; avoid PCM behind known hot-spot-prone regions.
   c) Prefer shape-stabilized organics or thoroughly sealed macrocapsules; apply foil facers on PV-facing sides to interrupt wicking paths.
   d) Implement temperature-aware inspection/monitoring (e.g., more frequent IR scans and connector checks at high-temperature sites).
iv. Standards and protection architecture (design-level mitigations): recommended practice is to prefer ungrounded architectures with Insulation Monitoring Devices (IMD) and DC-sensitive Residual-Current monitoring/detection (RCM/RCD), or, if grounded arrays are used, to combine IMD + DC-sensitive RCM and avoid blind spots; these choices are discussed alongside NEC/UL 1741 and IEC 60364–7/IEC 62257–7 contexts. Routine O&M (IR thermography; connector integrity; correct mating/torque) reduces hot-spot and connector-fault incidence [83].

5.2. Cycling stability and degradation

Long-term PV–PCM performance depends on how the PCM and its package tolerate repeated melting/solidification. Evidence from realistic cycling experiments and field-scale units shows three main themes:

(1) Enthalpy and phase-temperature drift depend strongly on exposure to air and sealing quality [84]: Macro-encapsulated PCMs cycled under ambient air show much larger losses in latent heat and noticeable shifts of melting/solidification peaks compared with inert or well-sealed configurations. In welded spheres (no air exposure), one study reports a ΔH decreased of ~ 24.5 % (melting) and 16 % (solidification) after 60 cycles for D-mannitol; with minor/low sealing, losses rise and melting peaks shift to lower T; different suppliers exhibit 24.5 % vs 38.9 % enthalpy decrease under the same cycling, underscoring supply variability. Supercooling is also less pronounced in macro-encapsulated samples than in milligram DSC pans.
(2) Not all systems degrade measurably in practice [85]: a real-scale paraffin PCM–air heat exchanger run over 3 years and 75 monitored cycles showed repetitive thermal behavior with no observed degradation in PCM properties, indicating that paraffin PCMs operated near room temperature, properly encapsulated and sealed, can maintain performance over many cycles.
(3) Multi-cycle operation can be improved by a boundary-condition strategy [85]: recent multi-cycle analyses demonstrate that temperature inversion/rotation strategies at the right time in the cycle can sustain higher heat-extraction rates; for eicosane and gallium, switching hot/cold walls before full melt improves subsequent cycle performance, with Marangoni convection playing a major role for high-Pr PCMs.

Implications for PV–PCM:

- Favor airtight encapsulation (macro-capsules, welded seams, barrier foils) and avoid oxygen ingress to limit enthalpy drift. Report sealing method and atmosphere [84].
- For paraffins near 25–45 °C, typical of PV back-layers, long-duration cycling under outdoor-like conditions can be stable when packaging is robust; nevertheless, document cycle count and enthalpy retention with DSC on extracted samples [86].
- Consider operational control (e.g., partial discharge or temperature inversion via flow or module orientation, where feasible) to avoid performance slow-down across cycles [85].

To reflect aging in simulations, the PCM's latent heat and phase-change temperature vary with the number of thermal cycles [84]. The variation can be modulated by a qualitative air-exposure/sealing indicator that represents packaging integrity (e.g., welded/hermetic vs. screw-cap or vented designs). For airtight packages, the indicator is set to negligible, so properties remain effectively constant over the simulated horizon. For packages with possible air ingress, the indicator is set to a non-zero value chosen to reproduce the enthalpy loss and peak-temperature drift observed in the supporting cycling tests (DSC or macro-scale). This cycle-aware parameterization can be applied without changing the structure of the enthalpy, effective-specific-heat, or lumped models, and enables scenario analyses of packaging choices and maintenance intervals. Table 4 consolidates the main degradation mechanisms observed under repeated melting/solidification—together with their risk conditions, the typical effects over cycles (e.g., latent-heat loss, shift of melting/solidification peaks, supercooling drift, leakage), and practical mitigations for PV–PCM modules.

The first column lists the mechanism/symptom (oxidation/air ingress, supercooling drift, packaging leakage, "no-degradation" cases under robust sealing, and multi-cycle performance slow-down). The second column details when the risk is highest (e.g., non-airtight caps or vented packs vs welded/hermetic encapsulation; PCM family and operating temperature range). The third column summarizes what typically changes with cycling (enthalpy retention, peak-temperature drift, stability, or repeatability of power). The fourth column provides actionable guidance (hermetic sealing, inert backfill, headspace management, use of nucleants where compatible, and simple operating strategies such as boundary inversion across cycles). Using Table 4 as a checklist is suggested when planning durability tests and when reporting data (including cycle count, sealing method/atmosphere, enthalpy retention, and any peak-temperature shift).

6. Major findings on PV-PCM systems from theoretical and experimental studies

This section presents a concise review of key findings and insights from significant publications in the field of PV-PCM technologies. Hasan et al. [35] conducted a study examining the utilization of various PCMs, specifically a eutectic PCM composed of capric-palmitic acid and the inorganic PCM salt hydrate $CaCl_2{\cdot}6H_2O$, within a rectangular container equipped with internal fins. The research was carried out in two distinct geographical locations: Dublin, Ireland, and Vehari, Pakistan. These locations represent different climate zones, allowing for an investigation into the impact of solar irradiation on the performance of the PV modules. In each location, three identical PV modules were deployed, with one module serving as a reference and the other two modules each enhanced with one of the selected PCMs. The experimental duration spanned 18 days in Dublin and 15 days in Vehari. The results of the temperature measurements for each PV module are illustrated in Fig. 12 [35].

It is evident that both locations exhibited a reduction in the temperature of the PV modules; however, the analysis extended beyond this observation. Hasan conducted an economic assessment, demonstrating that PV-PCM systems are not financially viable in colder climates, such as Ireland, while proving to be economically beneficial in hotter climates, such as Pakistan [2].

Another study conducted an annual global-scale simulation, revealing that PV-PCM systems consistently improve efficiency and electricity power output across various locations, with the exception of Antarctica [58]. The performance of PV-PCM systems was enhanced when the melting point of the PCM corresponded optimally to the climatic conditions, facilitating complete melting during daylight hours and subsequent solidification overnight. As highlighted by Fig. 13, PV-PCM systems exhibited their maximum potential in regions such as Africa, South Asia, Australia, and South and Central America, where solar irradiance is elevated and ambient temperatures remain high throughout the year. Despite the technical enhancements, the study also noted that PV-PCM systems may not be cost-effective in all locations, highlighting the need for further investigation to assess the cost-effectiveness of these systems.

An annual study on PV systems integrated with PCM revealed new challenges associated with the implementation of this cooling system [34]. The experimental study was conducted in the United Arab Emirates, characterized by hot climatic conditions. Observations indicated that during some summer nights, the PCM did not completely solidify, while similar issues were noted on colder winter days, which impeded the PCM from fully melting. These phenomena clearly hinder the efficient operation of PV-PCM systems; however, the study recorded a 10.5 °C reduction in PV module temperature and a 5.9 % increase in electrical energy output over the course of a year.

Khanna et al. developed a novel mathematical model for a tilted PV-PCM system, accounting for all three modes of heat transfer. The model examined the effects of tilt angle, wind azimuth angle (i.e., wind direction), wind velocity, ambient temperature, phase-change temperature, and various climatic conditions [61–63]. They found that increasing the tilt angle of the system leads to a decrease in the temperature of the PV module [61]. At very small tilt angles, the energy

Table 3
Modeling options for PV–PCM systems: physics, cost, limits, use cases, and representative references.

Model family	Physics captured	Indicative computational demand	Main limitations	Appropriate use cases	Representative refs
Enthalpy–porosity CFD (2D/3D)	Conduction + melt convection; side-wall losses; geometry	High (hours–days for multi-hour transients)	Mushy-zone tuning; stiffness; risk of non-rigid "solid" motion if viscosity trick is mis-set	Thick PCM; fins/foams; tilt/wind; non-1D effects	[61,76]
Effective specific heat/ 1D FDM	Through-thickness conduction with latent heat via $c_A(T)$	Low–moderate (seconds–minutes)	No convection; sensitivity to ΔT; no lateral losses/fins	Thin/encapsulated PCM; BIPV back layers; early design	[61,77]
Lumped/thermal-network (PV/T-PCM)	System-level U values across solid/mushy/liquid + 5-parameter PV	Very low (seconds); ~14 s vs ~ 16 h CFD	Needs U parameterization; no internal fields	Rapid scans, design charts, controls, TEA	[57]

transfer within the PCM is primarily limited by convection, resulting in minimal energy flow (as shown in Fig. 14). This is largely due to the low thermal conductivity of the PCM, which restricts energy extraction from the PV panel. As the tilt angle increases, the convective energy flow within the PCM becomes more significant, enhancing energy extraction from the PV system and consequently lowering the PV temperature.

Khanna et al. also studied the effect of wind velocity, illustrating the relationship between the optimal depth of the PCM container and varying wind velocities across different daily solar radiation levels [63]. It is observed from Fig. 15 that the optimal depth decreases with increasing wind velocity. At lower wind velocities, heat losses are reduced, allowing for a higher rate of heat extraction by the PCM, leading to faster melting. Consequently, a larger volume of PCM is necessary to effectively cool the PV panel for the desired duration under lower wind velocity conditions.

An experimental study conducted by Maghrabie et al. aimed to record and analyze various indicators of the PV-PCM system, including temperature distribution, electrical power output, and electrical efficiency [68]. In this experiment, identical PV modules were utilized: one served as a conventional reference PV module (PVr), while the other was enhanced with a PCM container of varying thicknesses (10 mm, 20 mm, and 30 mm). As anticipated, the utilization of a PV-PCM system resulted in a reduction in module temperature distribution, leading to higher electrical power output and efficiency. Detailed results of temperature distribution were obtained using infrared cameras, as illustrated in Fig. 16. The findings indicated that the highest temperature was maintained in the upper section of the PV-PCM module, confirming that this area experienced less cooling due to the melting of the PCM, which subsequently slid downwards owing to the tilt angle.

The module stands were designed to be adjustable, allowing for the investigation of the effects of various tilt angles (15°, 20°, 25°, and 30°) on performance. The results indicated that the configuration with a tilt angle of 30° exhibited superior performance relative to the other tilt angles assessed. Additionally, it was observed that the 30 mm thickness of the PCM container outperformed both the 10 mm and 20 mm thicknesses. Fig. 17 illustrates the average electrical power output and average electrical efficiency for the different configurations analyzed [68].

In a research by Sharaf et al., a year-round performance of a PV system integrated with a PCM/aluminum metal foam (PCM/AMF) composite as a passive cooling solution was developed utilizing data collected on-site [65]. Experiments were carried out during various months to compare the performance of the proposed PV-PCM/AMF system with traditional PV systems and PV-PCM systems without metal foam, focusing on energy assessments. The results shown in Fig. 18 suggested that the PV-PCM/AMF configuration has the potential to serve as an effective thermal regulation technology for maintaining optimal temperatures in PV cells. Quantitatively, it was noted that the annual electrical power output of the PV-PCM and PV-PCM/AMF configurations increased by 4.5 % and 6.4 %, respectively, in comparison to the traditional PV system. The results indicated that the highest percentage increase in daily average electrical efficiency occurred in July, with the PV electrical efficiency rising by 8.41 % and 13 % due to the integration of pure PCM and composite PCM, respectively. Conversely, the percentage gain in daily average electrical efficiency was lower in November, registering at 0.6 % for the PV-PCM and 1.03 % for the PV-PCM/AMF.

Arici et al. analyzed various PCMs with differing phase-change temperatures and latent heat of fusion to determine the most suitable PCM for the PV panel under specific climatic conditions of Ankara and Mersin [87]. The electricity generated by the analyzed PV-PCM configuration is illustrated in Fig. 19. In both cities, it is evident that the maximum increases in electricity output are relatively small, with the highest levels occurring in May.

Alwan et al. explored the effects of integrating a 4-cm-thick layer of paraffin wax as a PCM behind a crystalline silicon PV module to enhance efficiency by reducing thermal buildup [70]. Compared to a reference PV panel without PCM, the PV/PCM system achieved a higher power output, attributed to a lower back cell temperature of 3.2 °C, due to the heat absorption properties of the PCM.

As shown by Fig. 20, key findings reveal that under identical solar irradiation (728 W/m2), the PV/PCM panel produced 1.191 W more power than the non-PCM panel. At peak conditions, with 961 W/m2 irradiance, the maximum power point (MPP) for the PV/PCM reached 45.887 W, outperforming the reference PV module's 42.887 W. This improvement was linked to the thermal regulation provided by the PCM, which reduced panel overheating and maintained optimal voltage at the MPP, resulting in enhanced electrical efficiency.

The study demonstrates that incorporating PCM into PV panels is an effective strategy to boost efficiency by managing operating temperatures.

In the investigation of PV-PCM systems, it was observed that in several studies, PCMs are integrated with PV/T systems, resulting in the formation of PV/T-PCM systems [59,60,71]. Additionally, aluminum metal foam (AMF) has been incorporated within the PCM, leading to the development of PV-PCM/AMF systems [56,65]. These modified systems have demonstrated enhanced performance relative to traditional PV-PCM configurations. For instance, a study conducted in Egypt indicated that the annual electrical power output of a PV-PCM system increased by 4.5 %, while the PV-PCM/AMF system exhibited an increase of 6.4 % when compared to conventional PV modules [21]. However, as these systems fall outside the primary focus of this work,

their introduction serves merely to highlight potential avenues for further investigation.

Very recently, two artificial neural network (ANN) models were trained and validated for performance prediction of PV and PV/T-PCM systems that incorporate water cooling and biocomposite PCMs through experimental and theoretical methods [71]. The spider graph in Fig. 21 indicates that the power generated by the PV system is significantly lower than that produced by the PV/T-PCM system. Additionally, the ANN models developed successfully captured the trends and predicted the output values with high accuracy.

Very recently, Zhou et al. used ANNs and group method of data handling techniques to create an accurate model for predicting the hourly temperature of the PV-PCM system [88]. The performance assessment of this model yielded R^2, RMSE, and MSE values of 0.97602, 1.483, and 2.22, respectively.

7. Environmental and economic analysis of PV-PCM systems

To this point, the publications reviewed have primarily focused on numerical models, numerical simulations, or experimental studies pertaining to the performance of PV-PCM systems. A noteworthy study conducted by Foteinis et al. investigated the environmental performance of PV-PCM systems using the life cycle assessment (LCA) methodology [68]. It was determined that the integration of PCM as a cooling system increased the total environmental footprint of a standalone ground-mounted solar PV system by 21.9 %. However, the electricity power output experienced an increase of approximately 9.4 % over the 25-year lifespan of the system. Furthermore, the incorporation of PCM extended the useful life of a PV module by at least 5 years, contributing positively to the environmental sustainability of the system.

The surplus electricity generated compared to conventional PV modules led to a reduced score in ecotoxicity and toxicity, which are significant concerns associated with PV technology. The additional electricity produced as a result of the PCM cooling system also enhanced the renewable energy share within the energy mix, making it more environmentally favorable than conventional standalone PV systems, particularly in the context of the study's location, which was primarily reliant on fossil fuels. This increased electricity output also mitigates the negative impacts commonly associated with land use and land use change, which are significant concerns for large-scale solar PV farms.

In summary, while the longer lifespan, enhanced electrical power output, and reduced land use may offset the initial environmental footprint of PCM cooling systems, the study suggested a shift toward more environmentally friendly materials, such as biobased PCMs.

The economics of PV-PCM systems are highly location-dependent, influenced by two primary factors:

- The costs associated with PCM, encapsulation materials, and manufacturing processes vary across different locations.
- Solar irradiance levels differ by location, affecting the overall electrical efficiency of the systems.

For reference, Hasan et al. employed identical PV-PCM systems in two distinct locations: Pakistan and Ireland. The research indicated that the system was economically feasible in Pakistan due to lower costs for manufacturing and encapsulation materials, combined with higher efficiency levels. In contrast, the same PV-PCM system was found to be economically unviable in Ireland [35].

Furthermore, Hasan conducted an Energy Payback Time (EPBT) assessment for a PV-PCM system located in the UAE, which utilized paraffin wax as the PCM. The initial EPBT was calculated to be 10 years. To improve cost-effectiveness, the author proposed substituting paraffin wax with salt hydrates, which significantly lowered the PCM price and resulted in a recalculated EPBT of only 3 years [34].

Radziemska et al. conducted a straightforward economic analysis for a 1 kW PV module. Their analysis indicated that the cost of a PV-PCM system was 8.5 % higher than that of conventional PV modules while generating 7 % more energy over the course of a year. Assuming a lifespan of 30 years for the PV-PCM system, the revenue from the excess energy produced results in a 10 % profit margin [60].

Table 4
Degradation mechanisms, risk conditions, effect over cycles, and mitigations for PV–PCM [84–86].

Mechanism/ symptom	Risk conditions	Effect over cycles	Mitigation/ reporting
Oxidation/air ingress	Non-airtight caps, voids, vented packs	Latent heat loss, melting/ solidification peaks shift to lower T; supplier variability	Welded or hermetic seals, inert backfill; log supplier/lot; DSC checks at 0/20/40/60 cycles
Supercooling drift	Certain organics (e.g., sugar alcohols)	Larger in DSC microsamples; less in spheres	Macro-encapsulation; nucleants if compatible
Packaging leakage/ tightness	Thermal expansion, poor sealing	Mass loss, capacity loss	Allow headspace where needed; robust seams; periodic mass check
"No-degradation" cases	Paraffin, near-ambient, proper sealing	Stable, repeatable power and timing over the years	Document test cycles; replicate in PV–PCM modules
Multi-cycle performance slow-down	Full melts with fixed boundaries	Reduced heat extraction in later cycles	Switch/invert boundaries at the onset of slow-down; orientation strategies

Notes. Latent-heat loss refers to the change in DSC-derived melting/solidification enthalpy; peak shift refers to the temperature of the main endo/exothermic peak. Enthalpy retention is the ratio of enthalpy after n cycles to the initial value. Hermetic/airtight implies welded seams or equivalent gas-tight seals; air ingress includes screw-cap, vented, or loosely sealed packages.

8. Conclusions

8.1. Final Remarks

The integration of PCMs into PV systems represents a substantial leap forward in solar energy technology by addressing one of the primary limitations of PV performance—thermal regulation. This passive cooling approach, requiring only an initial investment with no ongoing maintenance or additional costs, holds significant promise for improving PV efficiency, especially in high-irradiance regions where PV systems are most prone to overheating. By maintaining lower operational temperatures, PCMs demonstrate an impressive ability to enhance PV module efficiency and thus offer an economically advantageous solution for solar energy in hotter climates. Various cooling methods for PV systems have evolved, and recent advancements, such as the addition of nanoparticles to PCMs and the development of hybrid PV/T-PCM systems, have shown considerable potential in enhancing heat dissipation and optimizing energy output.

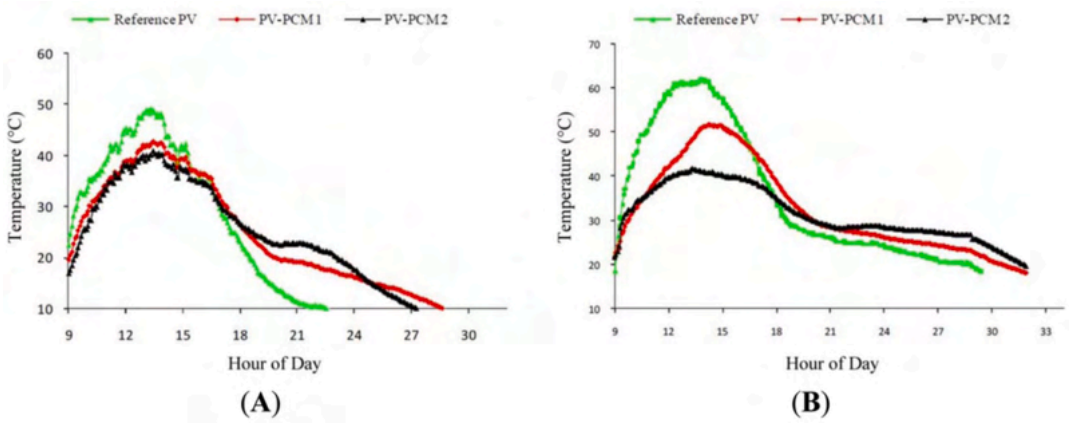

Fig. 12. PV module temperatures throughout the day in Dublin (A) and Vehari (B) [35].

A comprehensive literature review revealed notable progress in PV-PCM integration, including temperature control, efficiency improvements, and the unique material properties that contribute to these outcomes. A breakdown of the technical characteristics of PV systems used with PCMs provides further insights into the optimization of performance:

1. PV nominal power and nominal operating cell temperature (NOCT): The reviewed studies encompass PV systems with a power output range of 10 W to 305 W. When specified, these systems exhibit NOCT values between 45–47 °C.
2. Efficiency ranges: The nominal efficiency of PV systems previously combined with PCMs typically lies between 9.3 % and 17.3 %.
3. PCM types and thermal properties:
   - o PCM material types: organic PCMs, such as paraffin wax and proprietary formulations like RT25 and RT42, are most commonly used, followed by salt hydrates, including Calcium Chloride Hexahydrate ($CaCl_2{\cdot}6H_2O$), and eutectic mixtures like capric acid-palmitic acid blends.
   - o Phase-change temperatures: PCM phase-change temperatures span from as low as 5 °C up to 60 °C. Most organic PCMs melt within the range of 25–44 °C, making them well-suited for moderate to high-temperature PV environments where they can readily absorb and release heat as needed.
   - o Latent heat of fusion: this value, indicating the PCM's heat absorption capacity, generally ranges from 134 kJ/kg to 250 kJ/kg. Eutectic mixtures and salt hydrates, while typically offering higher latent heat, have shown potential applications in enhancing heat management due to their effective thermal properties.
   - o Thermal conductivity: the thermal conductivity of PCMs in their solid phase is relatively low, with values spanning from 0.14 to 1.09 W/mK. Salt hydrates generally offer higher conductivity compared to organic PCMs. Innovations like adding nanoparticles, metal foams, and fins have been shown to improve the thermal response of organic PCMs, making them more suitable for PV applications.
4. Integration techniques and system configurations: common attachment methods for PCMs include adhesive, glue, screwing, and thermal paste. PCM layer thicknesses typically vary between 10 mm and 50 mm. Adhesives and gluing methods are widely used due to their cost-effectiveness and efficient thermal transfer capabilities, while thermal paste is often applied to increase conductivity in systems with thicker PCM layers. The choice of integration method can influence both the thermal performance and structural durability of the PV-PCM system.

Numerous studies have shown that PCM integration can significantly increase energy output, with efficiency gains typically ranging from + 1 % to as high as + 14.4 % in some cases. In certain scenarios, PCM cooling has reduced PV module temperatures by up to 30 °C, leading to a more stable and efficient system performance. Research has been carried out in numerous locations worldwide, covering diverse climate zones. This broad range of climates highlights PCM technology's flexibility to adapt to various environmental conditions, while also pointing to research gaps, especially in areas with extreme temperature fluctuations or high humidity. Notably, PV-PCM systems are economically advantageous in regions with high irradiance, where cooling is most beneficial and power output gains are most pronounced. In contrast, PCM solutions in regions

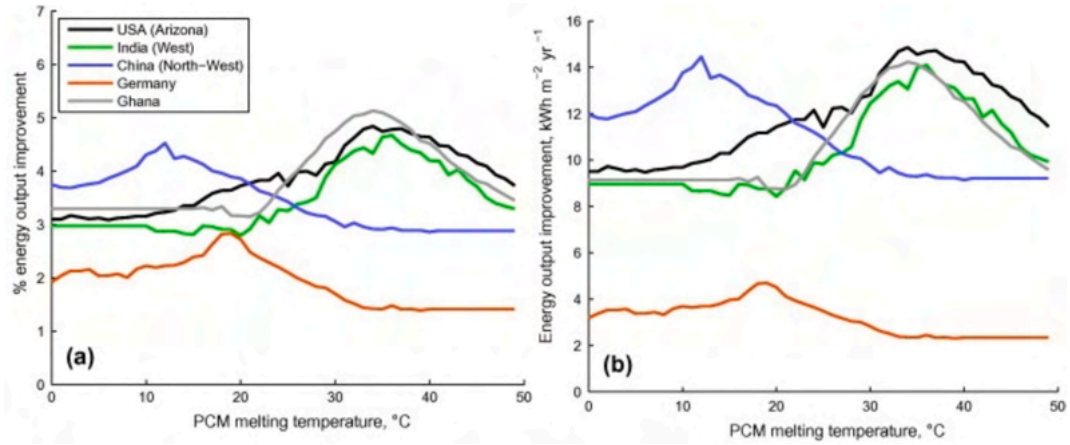

Fig. 13. The improvement in PV output as a function of PCM phase-change temperature [58].

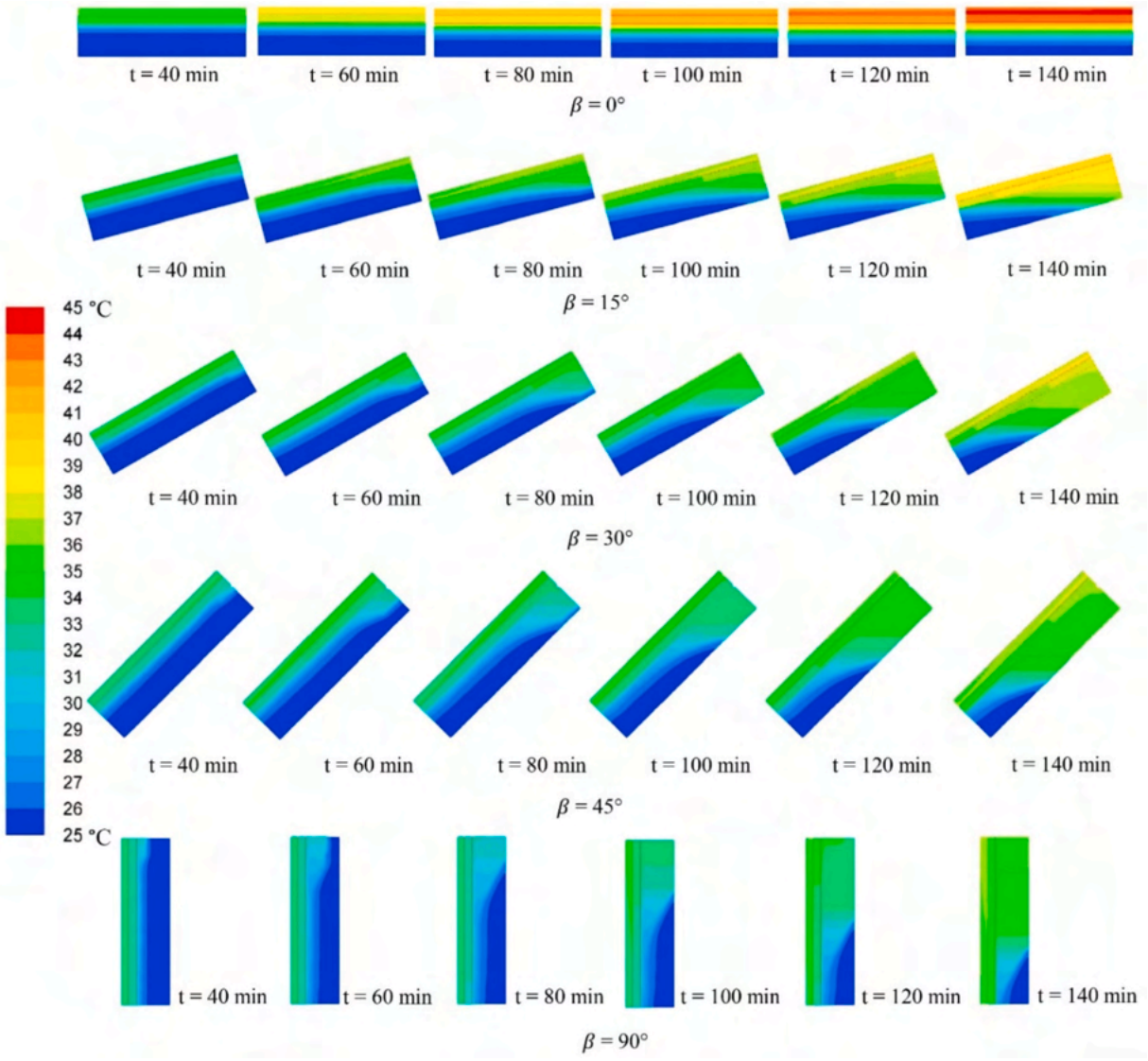

Fig. 14. Variation in the temperature of the PV-PCM system with time for various tilt angles of the system (β) [61].

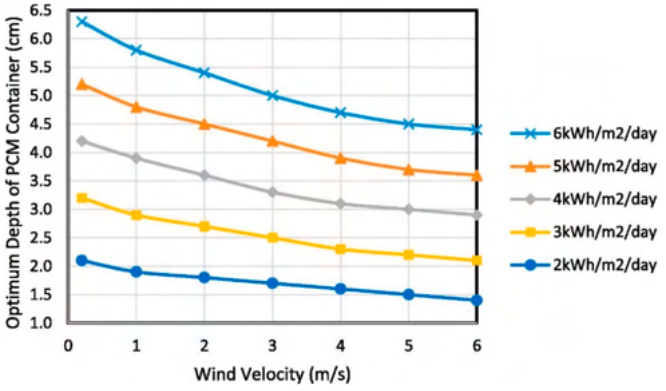

Fig. 15. Variation in the optimum depth of the PCM container with wind velocity for various solar radiation levels [63].

with fluctuating or moderate temperatures may offer limited economic returns. Cost analyses conducted across diverse regions, including Pakistan, Ireland, and the UAE, support these findings, suggesting that PV-PCM systems are best suited for sunny climates. In summary, PV-PCM systems are best suited for sunny climates, demonstrating the strongest economic potential where cooling benefits and power gains are most pronounced.

8.2. *Discussion and future research directions*

Building on the promising findings from existing studies, future work should address critical areas to advance PV-PCM technology further. To gain a comprehensive understanding of the long-term effectiveness of PV-PCM systems, it is essential to conduct annual experimental campaigns across diverse climates. These campaigns will provide valuable data, enabling a quantitative assessment of PCM's influence on PV systems' thermal regulation and electrical efficiency. Investigating the performance of various PCMs with different thicknesses and

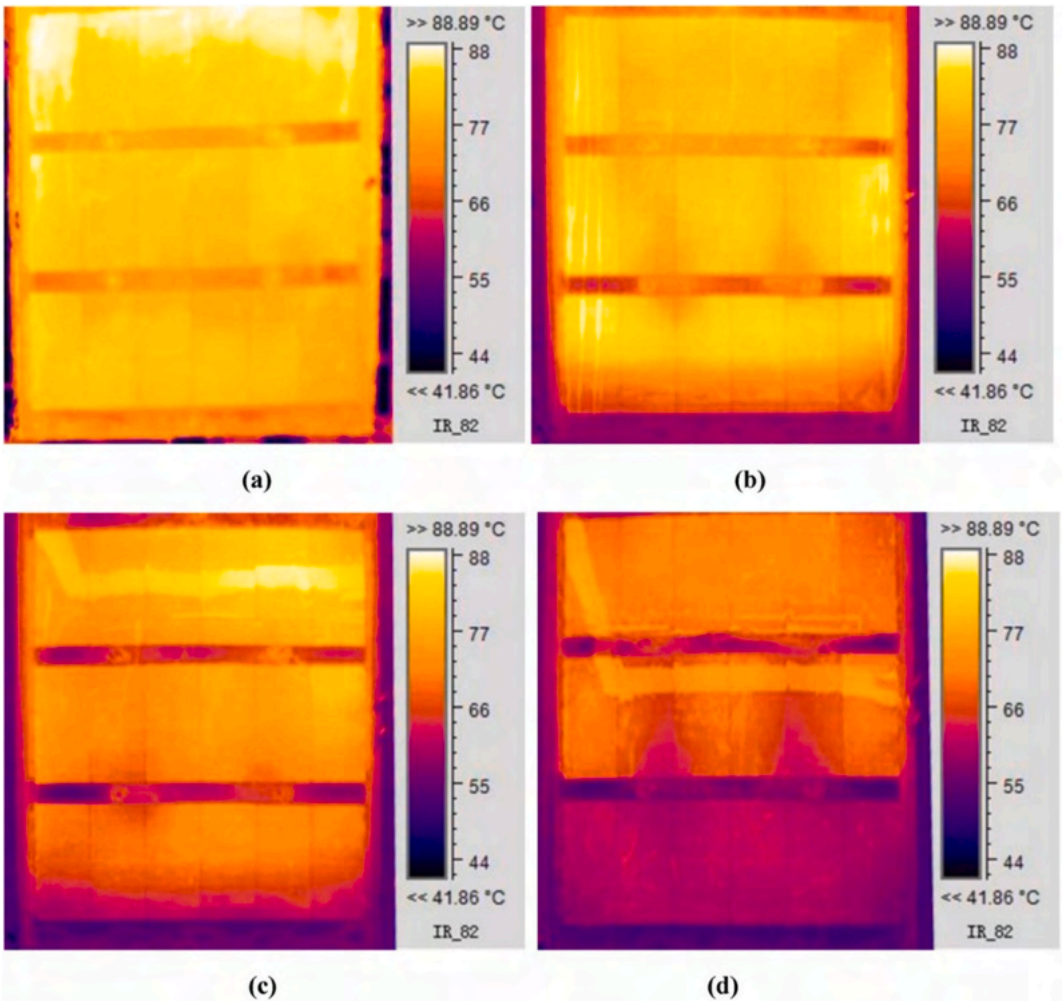

Fig. 16. Infrared camera thermal images at a tilt angle of 30° and 800 W/m2 for (a) PVr and PV- PCM with PCM thicknesses of (b) 1 cm, (c) 2 cm, and (d) 3 cm [68].

encapsulation methods will also be pivotal. This will reveal the real-world effectiveness of each PCM and allow for selecting the most suitable material configurations for specific climates, thereby maximizing the efficiency and cost-effectiveness of PV-PCM systems in targeted regions.

In parallel, developing detailed simulation models through advanced software, such as ANSYS, could offer a robust thermal and electrical model of PV-PCM systems, enhancing validation efforts for data collected from both experimental and field setups. These simulations will play a crucial role in predicting PV-PCM performance across different conditions, providing a comprehensive tool for optimizing material and design choices prior to practical implementation.

Additionally, further research into hybrid PV/T-PCM systems incorporating aluminum metal foam could prove particularly beneficial. Metal foams offer high thermal conductivity, which could significantly improve heat dissipation, providing enhanced performance without incurring substantial additional costs. This enhancement in thermal transfer could render PV-PCM systems even more effective and versatile in various climates, increasing their feasibility and durability over extended periods.

Long-term feasibility hinges on encapsulation integrity: welded/hermetic packages and inert atmospheres limit drift in latent heat and phase temperature, whereas air exposure can nearly double degradation rates under otherwise similar cycling. Multi-cycle temperature-inversion strategies may further sustain performance in service.

Future work should also prioritize several other challenges highlighted in this review:

a) Material stability and longevity: long-term studies are necessary to assess the durability and phase stability of PCM materials under prolonged cyclic heating. Addressing issues such as PCM leakage, degradation, and encapsulation integrity will be vital to ensure the sustained performance of PV-PCM systems.
b) Optimization of thermal conductivity: the inherently low thermal conductivity of PCMs, particularly in solid form, remains a limitation for efficient heat transfer. Continued research into PCM composites with embedded high-conductivity materials—such as graphite or metal nanoparticles—will be essential to achieving enhanced thermal performance without sacrificing latent heat capacity.
c) Environmental and economic viability: to reduce the environmental footprint, alternative PCM materials, especially those that are bio-based or sustainably sourced, should be explored. Expanding the use

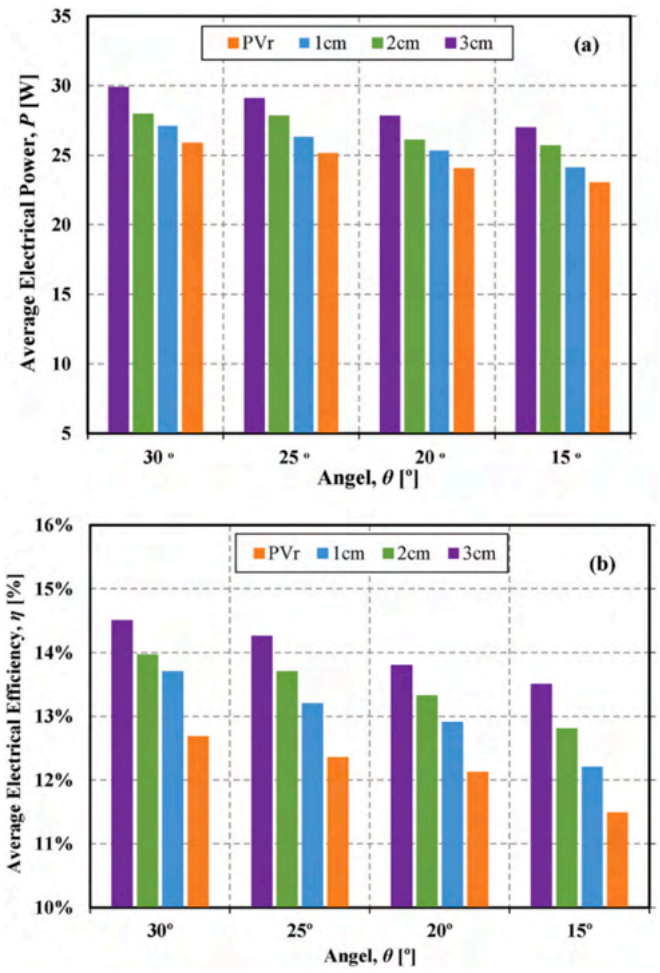

Fig. 17. For different tilt angles, (a) average electrical power output and (b) average electrical efficiency for the reference module and various thicknesses of PCM [68].

of eco-friendly PCMs can make PV-PCM technology more accessible and economically viable for widespread application.

d) Commercial-scale implementation: while simulation-based research has advanced understanding of PV-PCM systems, larger-scale experimental trials and in-depth economic feasibility studies are needed to support commercial adoption. Assessing the systems' energy-saving potential, cost-effectiveness, and market applicability will enable stakeholders to make informed decisions about scaling PV-PCM systems in commercial solar projects.

e) Climate- and season-aware phase-change temperature selection: material choice should ensure daytime activation and nocturnal reset: typical midday PV back-surface temperatures should lie ~ 5–15 °C above the phase-change temperature, with night-time minima ≥ 5–10 °C below it in the target season. For hot/arid sites, cascaded PCMs or slightly higher phase-change temperatures may be required; AI-based supervisory control can further manage activation/reset under variable weather.

f) Model development, verification, and validation: future studies should adopt clear V&V protocols (mesh/time-step independence for CFD; 1-D Stefan checks for conduction models; cross-validation to experiments for lumped networks) and report standard metrics (e.g., RMSE/NRMSE, MAE, r/R^2, runtime). Open datasets (boundary conditions, temperature time series) and benchmark cases will enable reproducible comparisons across modelling families.

g) Safety and risk engineering: because organic PCMs are combustible, PV-PCM designs should incorporate non-combustible barriers, adequate standoff from conductors and junction boxes, and shape-stabilised/encapsulated forms that limit leakage and fuel mobility. System-level protections (e.g., IMD with DC-sensitive RCM/RCD, careful use of GFPD where applicable) and temperature-aware inspection regimes should be integrated from the outset.

h) Reporting standards and data harmonisation: consistent indicators (ΔT, efficiency in %, absolute changes in percentage points, relative gains as %), clear phase-change temperature specification, climate/site metadata, and data availability statements should be required to enable *meta*-analysis and design translation.

i) Expanding future methodologies to include multi-objective optimization (ΔT/EEP vs. mass/LCOE/fire risk), cradle-to-grave LCA (including end-of-life and safety), and hybrid physics-informed AI modeling with standardized validation.

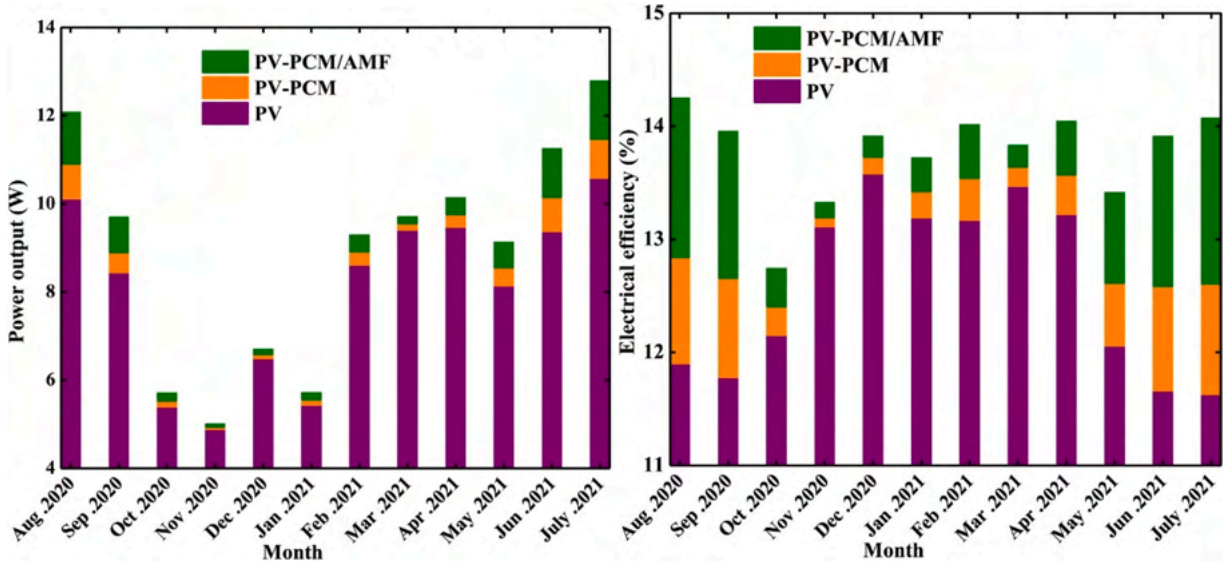

Fig. 18. Average PV power output and electrical efficiency for a typical day of each month [65].

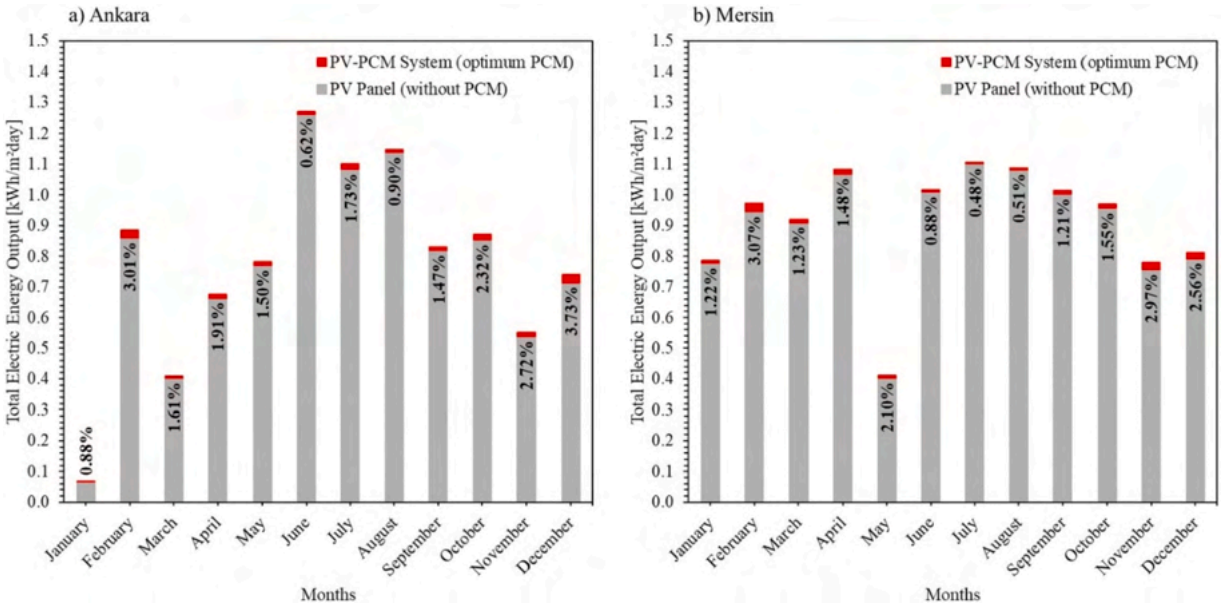

Fig. 19. Improvement in total electric energy output by coupling PCM to PV system, a) Ankara and b) Mersin [87].

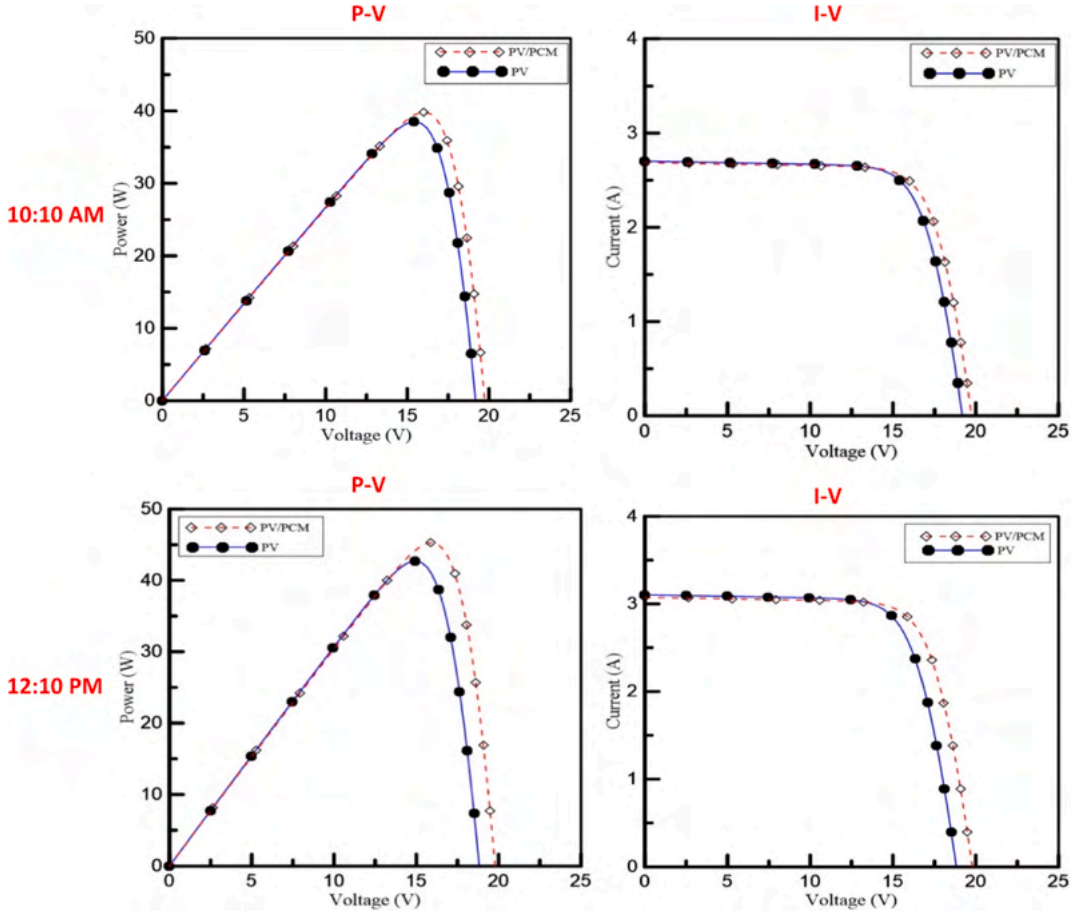

Fig. 20. P–V and I–V curves for PV and PV/PCM [70].

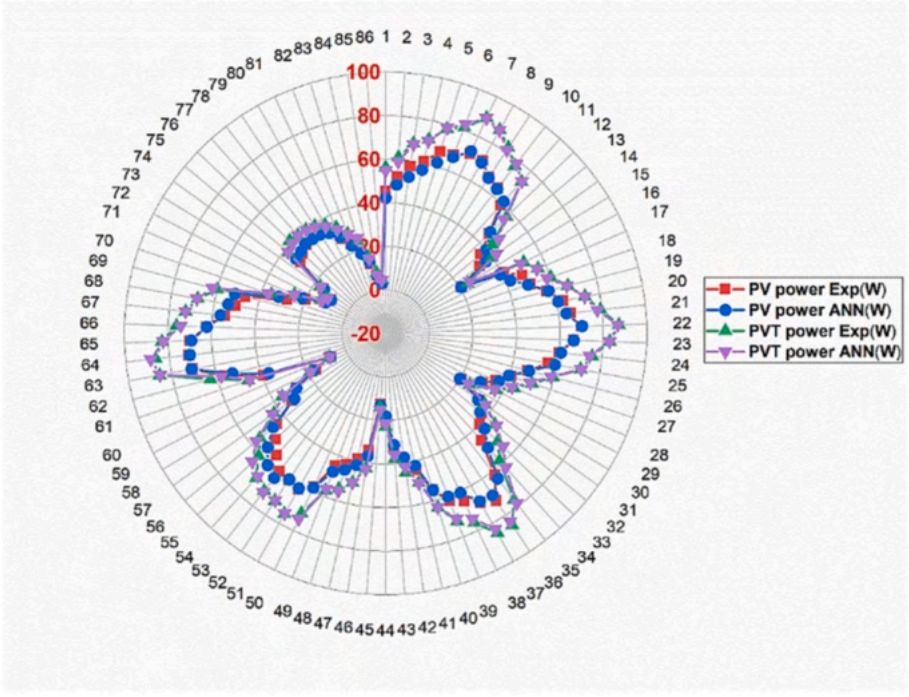

(a)

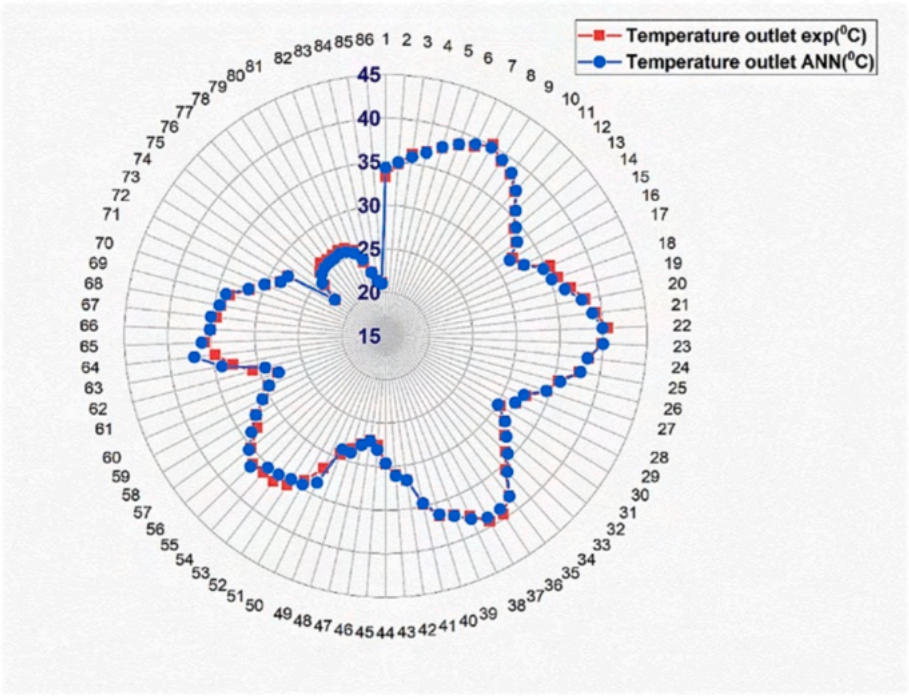

(b)

Fig. 21. Comparison plot between: (a) Power output of PV (experimental), Power output of PV (ANN), Power output of PV/T (experimental), Power output of PV/T (ANN); (b) PV/T temperature outlet (experimental) vs PV/T temperature outlet (ANN) [71].

By focusing on these areas, future research can address the current limitations of PV-PCM technology, paving the way for this solution to become a robust and sustainable component in the global solar energy landscape. Addressing these challenges will maximize the efficiency, durability, and environmental sustainability of PV-PCM technology, helping to establish it as an effective and scalable solution for efficient and sustainable solar energy generation worldwide.

CRediT authorship contribution statement

Domenico Mazzeo: Writing – review & editing, Writing – original draft, Visualization, Validation, Software, Resources, Methodology, Investigation, Formal analysis, Data curation, Conceptualization. **Luigi Pietro Maria Colombo:** Writing – review & editing, Visualization, Validation, Resources, Investigation, Formal analysis. **Sonia Leva:** Writing – review & editing, Visualization, Resources, Project administration, Funding acquisition, Formal analysis.

Declaration of competing interest

D. Mazzeo and L. P. M. Colombo serve as Guest Editors for this Special Issue and had no role in the peer review or editorial decision for this manuscript. In accordance with the journal's policy, this manuscript was handled by independent editors. All authors declare no additional competing interests.

Acknowledgments

This study was conducted within the Agritech National Research Center and received funding from the European Union Next-GenerationEU (Piano Nazionale di Ripresa e Resilienza (PNRR) – Missione 4 Componente 2, Investimento 1.4 – D.D. 1032 17/06/2022, CN00000022). This manuscript reflects only the authors' views and opinions, neither the European Union nor the European Commission can be considered responsible for them.

Data availability

Data will be made available on request.

References

[1] Karunesh Kant, A. Shukla, Atul Sharma, Pascal Henry Biwole, Heat transfer studies of photovoltaic panel coupled with phase change material, Solar Energy, Volume 140, 2016, Pages 151-161, ISSN 0038-092X, Doi: 10.1016/j.solener.2016.11.006.

[2] Karunesh Kant, A. Shukla, Atul Sharma, Pascal Henry Biwole, Thermal response of poly-crystalline silicon photovoltaic panels: Numerical simulation and experimental study, Solar Energy, Volume 134, 2016, Pages 147-155, ISSN 0038-092X, Doi: 10.1016/j.solener.2016.05.002.

[3] Peter Atkin, Mohammed M. Farid, Improving the efficiency of photovoltaic cells using PCM infused graphite and aluminium fins, Solar Energy, Volume 114, 2015, Pages 217-228, ISSN 0038-092X, Doi: 10.1016/j.solener.2015.01.037.

[4] C.S. Malvi, D.W. Dixon-Hardy, R. Crook, Energy balance model of combined photovoltaic solar-thermal system incorporating phase change material, Solar Energy, Volume 85, Issue 7, 2011, Pages 1440-1446, ISSN 0038-092X, Doi: 10.1016/j.solener.2011.03.027.

[5] J. K. Tonui, Y. Tripanagnostopoulos, Air-cooled PV/T solar collectors with low-cost performance improvements, Solar Energy, Volume 81, Issue 4, 2007, Pages 498-511, ISSN 0038-092X, Doi: 10.1016/j.solener.2006.08.002.

[6] E. Radziemska, The effect of temperature on the power drop in crystalline silicon solar cells, Renewable Energy, Volume 28, Issue 1, 2003, Pages 1-12, ISSN 0960-1481, Doi: 10.1016/S0960-1481(02)00015-0.

[7] E. Radziemska, E. Klugmann, Thermally affected parameters of the current-voltage characteristics of silicon photocell, Energy Conversion and Management, Volume 43, Issue 14, 2002, Pages 1889-1900, ISSN 0196-8904, Doi: 10.1016/S0196-8904(01)00132-7.

[8] George Makrides, Bastian Zinsser, George E. Georghiou, Markus Schubert, Jürgen H. Werner, Temperature behaviour of different photovoltaic systems installed in Cyprus and Germany, Solar Energy Materials and Solar Cells, Volume 93, Issue 6, 2009, Pages 1095-1099, ISSN 0927-0248, Doi: 10.1016/j.solmat.2008.12.024.

[9] Yasser Fathi Nassar, Abubaker Awidat Salem, The reliability of the photovoltaic utilization in southern cities of Libya, Desalination, Volume 209, Issue 1, 2007, Pages 86-90, ISSN 0011-9164, Doi: 10.1016/j.desal.2007.04.013.

[10] Y. Du, C.J. Fell, B. Duck, D. Chen, K. Liffman, Y. Zhang, M. Gu, Y. Zhu, Evaluation of photovoltaic panel temperature in realistic scenarios, Energy Conversion and Management 108 (2016) 60–67, https://doi.org/10.1016/j.enconman.2015.10.065.

[11] Tao Ma, Hongxing Yang, Yinping Zhang, Lin Lu, and Xin Wang. Using phase change materials in photovoltaic systems for thermal regulation and electrical efficiency improvement: A review and outlook. Renewable and Sustainable Energy Reviews, Volume 43, 2015, Pages 1273–1284, ISSN 1364-0321, Doi: 10.1016/j.rser.2014.12.003.

[12] Stefan Krauter. Increased electrical yield via water flow over the front of photovoltaic panels. Solar Energy Materials and Solar Cells, Volume 82, 2004, Pages 131–137, ISSN 0927-0248, Doi: 10.1016/j.solmat.2004.01.011.

[13] Earle Wilson. Theoretical and operational thermal performance of a 'wet' crystalline silicon PV module under Jamaican conditions. Renewable Energy, Volume 34, 2009, Pages 1655–1660, ISSN 0960-1481, Doi: 10.1016/j.renene.2008.10.024.

[14] Kaoru Furushima and Yutaka Nawata. Performance evaluation of photovoltaic power-generation system equipped with a cooling device utilizing siphonage. Journal of Solar Energy Engineering, Volume 128, 2005, Pages 146–151, ISSN 0199-6231, Doi: 10.1115/1.2183805.

[15] J.K. Tonui and Y. Tripanagnostopoulos. Air-cooled PV/T solar collectors with low cost performance improvements. Solar Energy, Volume 81, 2007, Pages 498–511, ISSN 0038-092X, Doi: 10.1016/j.solener.2006.08.002.

[16] J.K. Tonui and Y. Tripanagnostopoulos. Improved PV/T solar collectors with heat extraction by forced or natural air circulation. Renewable Energy, Volume 32, 2007, Pages 623–637, ISSN 0960-1481, Doi: 10.1016/j.renene.2006.03.006.

[17] Tapas K. Mallick, Philip C. Eames, and Brian Norton. Using air flow to alleviate temperature elevation in solar cells within asymmetric compound parabolic concentrators. Solar Energy, Volume 81, 2007, Pages 173–184, ISSN 0038-092X, Doi: 10.1016/j.solener.2006.04.003.

[18] H.X. Yang, R.H. Marshall, and B.J. Brinkworth. Validated simulation for thermal regulation of photovoltaic wall structures. Conference Record of the Twenty Fifth IEEE Photovoltaic Specialists Conference - 1996, 1996, Pages 1453–1456, ISSN 0160-8371, Doi: 10.1109/PVSC.1996.564409.

[19] B.J. Brinkworth and M. Sandberg. Design procedure for cooling ducts to minimise efficiency loss due to temperature rise in PV arrays. Solar Energy, Volume 80, 2006, Pages 89–103, ISSN 0038-092X, Doi: 10.1016/j.solener.2005.05.020.

[20] B.J. Brinkworth. Estimation of flow and heat transfer for the design of PV cooling ducts. Solar Energy, Volume 69, 2000, Pages 413–420, ISSN 0038-092X, Doi: 10.1016/S0038-092X(00)00082-7.

[21] S. Sargunanathan, A. Elango, and S. Tharves Mohideen. Performance enhancement of solar photovoltaic cells using effective cooling methods: A review. Renewable and Sustainable Energy Reviews, Volume 64, 2016, Pages 382–393, ISSN 1364-0321, Doi: 10.1016/j.rser.2016.06.024.

[22] A. Akbarzadeh and T. Wadowski. Heat pipe-based cooling systems for photovoltaic cells under concentrated solar radiation. Applied Thermal Engineering, Volume 16, 1996, Pages 81–87, ISSN 1359-4311, Doi: 10.1016/1359-4311(95)00012-3.

[23] Erdem Cuce, Tulin Bali, and Suphi Anil Sekucoglu. Effects of passive cooling on performance of silicon photovoltaic cells. International Journal of Low-Carbon Technologies, Volume 6, 2011, Pages 299–308, ISSN 1748-1317, Doi: 10.1093/ijlct/ctr018.

[24] Adeel Waqas, Jie Ji, Lijie Xu, Majid Ali, Zeashan, Jahanzeb Alvi, Thermal and electrical management of photovoltaic panels using phase change materials – A review, Renewable and Sustainable Energy Reviews, Volume 92, 2018, Pages 254-271, ISSN 1364-0321, Doi: 10.1016/j.rser.2018.04.091.

[25] Sajan Preet, Water and phase change material based photovoltaic thermal management systems: A review, Renewable and Sustainable Energy Reviews, Volume 82, Part 1, 2018, Pages 791-807, ISSN 1364-0321, Doi: 10.1016/j.rser.2017.09.021.

[26] Tao Ma, Zhenpeng Li, Jiaxin Zhao, Photovoltaic panel integrated with phase change materials (PV-PCM): technology overview and materials selection, Renewable and Sustainable Energy Reviews, Volume 116, 2019, 109406, ISSN 1364-0321, Doi: 10.1016/j.rser.2019.109406.

[27] Taher Maatallah, Richu Zachariah, and Fahad Gallab Al-Amri. Exergo-economic analysis of a serpentine flow type water based photovoltaic thermal system with phase change material (PVT-PCM/water). Solar Energy, Volume 193, 2019, Pages 195–204, ISSN 0038-092X, Doi: 10.1016/j.solener.2019.09.063.

[28] Mohamed S. Yousef and Hamdy Hassan. Assessment of different passive solar stills via exergoeconomic, exergoenvironmental, and exergoenviroeconomic approaches: A comparative study. Solar Energy, Volume 182, 2019, Pages 316–331, ISSN 0038-092X, Doi: 10.1016/j.solener.2019.02.042.

[29] Mohamed S. Yousef and Hamdy Hassan. Energetic and exergetic performance assessment of the inclusion of phase change materials (PCM) in a solar distillation system. Energy Conversion and Management, Volume 179, 2019, Pages 349–361, ISSN 0196-8904, Doi: 10.1016/j.enconman.2018.10.078.

[30] Mohamed S. Yousef and Hamdy Hassan. An experimental work on the performance of single slope solar still incorporated with latent heat storage system in hot climate conditions. Journal of Cleaner Production, Volume 209, 2019, Pages 1396–1410, ISSN 0959-6526, Doi: 10.1016/j.jclepro.2018.11.120.

[31] Mohamed S. Sharaf and Mohamed Yousef. Review of cooling techniques used to enhance the efficiency of photovoltaic power systems. Environmental Science and Pollution Research, Volume 29, 2022, Pages 299–308, ISSN 1614-7499, Doi: 10.1007/s11356-022-18719-9.

[32] Mohamed S. Yousef, Mohamed Sharaf, and A.S. Huzayyin. Energy, exergy, economic, and enviroeconomic assessment of a photovoltaic module incorporated

with a paraffin-metal foam composite: An experimental study. Energy, Volume 238, 2022, Article 121807, ISSN 0360-5442, Doi: 10.1016/j.energy.2021.121807.
[33] A. Hasan, S.J. McCormack, M.J. Huang, and B. Norton. Characterization of phase change materials for thermal control of photovoltaics using differential scanning calorimetry and temperature history method. Energy Conversion and Management, Volume 81, 2014, Pages 322–329, ISSN 0196-8904, Doi: 10.1016/j.enconman.2014.02.042.
[34] A. Hasan, J. Sarwar, H. Alnoman, S. Abdelbaqi, Yearly energy performance of a photovoltaic-phase change material (PV-PCM) system in hot climate, Solar Energy, Volume 146, 2017, Pages 417-429, ISSN 0038-092X, Doi: 10.1016/j.solener.2017.01.070.
[35] A. Hasan, S.J. McCormack, M.J. Huang, B. Norton, Energy and Cost Saving of a Photovoltaic-Phase Change Materials (PV-PCM) System through Temperature Regulation and Performance Enhancement of Photovoltaics, Energies 7 (3) (2014) 1318–1331, https://doi.org/10.3390/en7031318.
[36] Rok Stropnik, Uroš Stritih, Increasing the efficiency of PV panel with the use of PCM, Renewable Energy, Volume 97, 2016, Pages 671-679, ISSN 0960-1481, Doi: 10.1016/j.renene.2016.06.011.
[37] Farouk Hachem, Bakri Abdulhay, Mohamad Ramadan, Hicham El Hage, Mostafa Gad El Rab, Mahmoud Khaled, Improving the performance of photovoltaic cells using pure and combined phase change materials – Experiments and transient energy balance, Renewable Energy, Volume 107, 2017, Pages 567-575, ISSN 0960-1481, Doi: 10.1016/j.renene.2017.02.032.
[38] Ahmad Hasan, Hamza Alnoman, and Yasir Rashid. Impact of integrated photovoltaic-phase change material system on building energy efficiency in hot climate. Energy and Buildings, Volume 130, 2016, Pages 495–505, ISSN 0378-7788, Doi: 10.1016/j.enbuild.2016.08.059.
[39] H. Fayaz, N.A. Rahim, M. Hasanuzzaman, R. Nasrin, and A. Rivai. Numerical and experimental investigation of the effect of operating conditions on performance of PVT and PVT-PCM. Renewable Energy, Volume 143, 2019, Pages 827–841, ISSN 0960-1481, Doi: 10.1016/j.renene.2019.05.041.
[40] Maria C. Browne, Brian Norton, and Sarah J. McCormack. Heat retention of a photovoltaic/thermal collector with PCM. Solar Energy, Volume 133, 2016, Pages 533–548, ISSN 0038-092X, Doi: 10.1016/j.solener.2016.04.024.
[41] Ali Hassan, Abdul Wahab, Muhammad Arslan Qasim, Muhammad Mansoor Janjua, Muhammad Aon Ali, Hafiz Muhammad Ali, Tufail Rehman Jadoon, Ejaz Ali, Ahsan Raza, and Noshairwan Javaid. Thermal management and uniform temperature regulation of photovoltaic modules using hybrid phase change materials-nanofluids system. Renewable Energy, Volume 145, 2020, Pages 282–293, ISSN 0960-1481, Doi: 10.1016/j.renene.2019.05.130.
[42] Mohamed S. Yousef, Hamdy Hassan, S. Kodama, and H. Sekiguchi. An experimental study on the performance of single slope solar still integrated with a PCM-based pin-finned heat sink. Energy Procedia, Volume 156, 2019, Pages 100–104, ISSN 1876-6102, Doi: 10.1016/j.egypro.2018.11.102. 5th International Conference on Power and Energy Systems Engineering (CPESE 2018).
[43] Lippong Tan, Abhijit Date, Gabriel Fernandes, Baljit Singh, and Sayantan Ganguly. Efficiency gains of photovoltaic system using latent heat thermal energy storage. Energy Procedia, Volume 110, 2017, Pages 83–88, ISSN 1876-6102, Doi: 10.1016/j.egypro.2017.03.110. 1st International Conference on Energy and Power, ICEP2016, 14-16 December 2016, RMIT University, Melbourne, Australia.
[44] Rajan Kumar, Paidi Praveen, Samikhshak Gupta, Juttu Saikiran, and Rabinder Singh Bharj. Performance evaluation of photovoltaic module integrated with phase change material-filled container with external fins for extremely hot climates. Journal of Energy Storage, Volume 32, 2020, Article 101876, ISSN 2352-152X, Doi: 10.1016/j.est.2020.101876.
[45] Muhammad Arslan Qasim, Hafiz Muhammad Ali, Muhammad Niaz Khan, Nauman Arshad, Danyal Khaliq, Zarghoon Ali, and Muhammad Mansoor Janjua. The effect of using hybrid phase change materials on thermal management of photovoltaic panels – an experimental study. Solar Energy, Volume 209, 2020, Pages 415–423, ISSN 0038-092X, Doi: 10.1016/j.solener.2020.09.027.
[46] S.A. Nada, D.H. El-Nagar, and H.M.S. Hussein. Improving the thermal regulation and efficiency enhancement of PCM-integrated PV modules using nanoparticles. Energy Conversion and Management, Volume 166, 2018, Pages 735–743, ISSN 0196-8904, Doi: 10.1016/j.enconman.2018.04.035.
[47] Ali H.A. Al-Waeli, K. Sopian, Miqdam T. Chaichan, Hussein A. Kazem, Adnan Ibrahim, Sohif Mat, and Mohd Hafidz Ruslan. Evaluation of the nanofluid and nano-PCM based photovoltaic thermal (PVT) system: An experimental study. Energy Conversion and Management, Volume 151, 2017, Pages 693–708, ISSN 0196-8904, Doi: 10.1016/j.enconman.2017.09.032.
[48] Leila Siahkamari, Masoud Rahimi, Neda Azimi, and Maysam Banibayat. Experimental investigation on using a novel phase change material (PCM) in microstructure photovoltaic cooling system. International Communications in Heat and Mass Transfer, Volume 100, 2019, Pages 60–66, ISSN 0735-1933, Doi: 10.1016/j.icheatmasstransfer.2018.12.020.
[49] Juan Duan and Fan Li. Transient heat transfer analysis of phase change material melting in metal foam by experimental study and artificial neural network. Journal of Energy Storage, Volume 33, 2021, Article 102160, ISSN 2352-152X, Doi: 10.1016/j.est.2020.102160.
[50] Xue Chen, Xiaolei Li, Xinlin Xia, Chuang Sun, and Rongqiang Liu. Thermal storage analysis of a foam-filled PCM heat exchanger subjected to fluctuating flow conditions. Energy, Volume 216, 2021, Article 119259, ISSN 0360-5442, Doi: 10.1016/j.energy.2020.119259.
[51] Huanpei Zheng, Changhong Wang, Qingming Liu, Zhongxuan Tian, and Xianbo Fan. Thermal performance of copper foam/paraffin composite phase change material. Energy Conversion and Management, Volume 157, 2018, Pages 372–381, ISSN 0196-8904, Doi: 10.1016/j.enconman.2017.12.023.
[52] Abdulmunem R. Abdulmunem, Pakharuddin Mohd Samin, Hasimah Abdul Rahman, Hashim A. Hussien, and Izhari Izmi Mazali. Enhancing PV cell's electrical efficiency using phase change material with copper foam matrix and multi-walled carbon nanotubes as passive cooling method. Renewable Energy, Volume 160, 2020, Pages 663–675, ISSN 0960-1481, Doi: 10.1016/j.renene.2020.07.037.
[53] Mohammad Amin Vaziri Rad, Alibakhsh Kasaeian, Soroush Mousavi, Fatemeh Rajaee, and Amir Kouravand. Empirical investigation of a photovoltaic-thermal system with phase change materials and aluminum shavings porous media. Renewable Energy, Volume 167, 2021, Pages 662–675, ISSN 0960-1481, Doi: 10.1016/j.renene.2020.11.135.
[54] Torsten Klemm, Abdelhakim Hassabou, Amir Abdallah, and Olaf Andersen. Thermal energy storage with phase change materials to increase the efficiency of solar photovoltaic modules. Energy Procedia, Volume 135, 2017, Pages 193–202, ISSN 1876-6102, Doi: 10.1016/j.egypro.2017.09.502. 11th International Renewable Energy Storage Conference, IRES 2017, 14-16 March 2017, Düsseldorf, Germany.
[55] M.A. Kibria, R. Saidur, F.A. Al-Sulaiman, Md Maniruzzaman A. Aziz, Development of a thermal model for a hybrid photovoltaic module and phase change materials storage integrated in buildings, Solar Energy, Volume 124, 2016, Pages 114-123, ISSN 0038-092X, Doi: 10.1016/j.solener.2015.11.027.
[56] Mohamed Sharaf, A.S. Huzayyin, Mohamed S. Yousef, Performance enhancement of photovoltaic cells using phase change material (PCM) in winter, Alexandria Engineering Journal, Volume 61, Issue 6, 2022, Pages 4229-4239, ISSN 1110-0168, Doi: 10.1016/j.aej.2021.09.044.
[57] Hussein M. Taqi Al-Najjar, Jasim M. Mahdi, Novel mathematical modeling, performance analysis, and design charts for the typical hybrid photovoltaic/phase-change material (PV/PCM) system, Applied Energy, Volume 315, 2022, 119027, ISSN 0306-2619, Doi: 10.1016/j.apenergy.2022.119027.
[58] Christopher J. Smith, Piers M. Forster, Rolf Crook, Global analysis of photovoltaic energy output enhanced by phase change material cooling, Applied Energy, Volume 126, 2014, Pages 21-28, ISSN 0306-2619, Doi: 10.1016/j.apenergy.2014.03.083.
[59] Zhenpeng Li, Tao Ma, Jiaxin Zhao, Aotian Song, Yuanda Cheng, Experimental study and performance analysis on solar photovoltaic panel integrated with phase change material, Energy, Volume 178, 2019, Pages 471-486, ISSN 0360-5442, Doi: 10.1016/j.energy.2019.04.166.
[60] Ewa Klugmann-Radziemska, Patrycja Wcisło-Kucharek, Photovoltaic module temperature stabilization with the use of phase change materials, Solar Energy, Volume 150, 2017, Pages 538-545, ISSN 0038-092X, Doi: 10.1016/j.solener.2017.05.016.
[61] Sourav Khanna, K.S. Reddy, Tapas K. Mallick, Performance analysis of tilted photovoltaic system integrated with phase change material under varying operating conditions, Energy, Volume 133, 2017, Pages 887-899, ISSN 0360-5442, Doi: 10.1016/j.energy.2017.05.150.
[62] Sourav Khanna, K.S. Reddy, Tapas K. Mallick, Climatic behaviour of solar photovoltaic integrated with phase change material, Energy Conversion and Management, Volume 166, 2018, Pages 590-601, ISSN 0196-8904, Doi: 10.1016/j.enconman.2018.04.056.
[63] Sourav Khanna, K.S. Reddy, Tapas K. Mallick, Optimization of solar photovoltaic system integrated with phase change material, Solar Energy, Volume 163, 2018, Pages 591-599, ISSN 0038-092X, Doi: 10.1016/j.solener.2018.01.002.
[64] A. Hasan, S.J. McCormack, M.J. Huang, J. Sarwar, B. Norton, Increased photovoltaic performance through temperature regulation by phase change materials: Materials comparison in different climates, Solar Energy, Volume 115, 2015, Pages 264-276, ISSN 0038-092X, Doi: 10.1016/j.solener.2015.02.003.
[65] Mohamed Sharaf, Mohamed S. Yousef, A.S. Huzayyin, Year-round energy and exergy performance investigation of a photovoltaic panel coupled with metal foam/phase change material composite, Renewable Energy, Volume 189, 2022, Pages 777-789, ISSN 0960-1481, Doi: 10.1016/j.renene.2022.03.071.
[66] A. Waqas, J. Ji, A. Bahadar, L. Xu, Zeshan, M. Modjinou, M., Thermal management of conventional photovoltaic module using phase change materials—An experimental investigation, Energy Exploration & Exploitation, Volume 37, Issue 5, 2019, Pages 1516-1540, Doi: 10.1177/0144598718795697.
[67] Hussein M. Maghrabie, A.S.A. Mohamed, Amany M. Fahmy, Ahmed A. Abdel Samee, Performance enhancement of PV panels using phase change material (PCM): An experimental implementation, Case Studies in Thermal Engineering, Volume 42, 2023, 102741, ISSN 2214-157X, Doi: 10.1016/j.csite.2023.102741.
[68] Spyros Foteinis, Nikolaos Savvakis, Theocharis Tsoutsos, Energy and environmental performance of photovoltaic cooling using phase change materials under the Mediterranean climate, Energy, Volume 265, 2023, 126355, ISSN 0360-5442, Doi: 10.1016/j.energy.2022.126355.
[69] K. B. Prakash, Manoj Kumar Pasupathi, Subramaniyan Chinnasamy, S. Saravanakumar, Murugesan Palaniappan, Abdulaziz Alasiri and M. Chandrasekaran, Energy and Exergy Enhancement Study on PV Systems with Phase Change Material, Sustainability, Volume 15, 2023, Article 3627, ISSN 2071-1050, Doi: 10.3390/su15043627.
[70] A.A. Alwan, A.M. Hassan, Experimental study on optimizing photovoltaic panel efficiency: harnessing paraffin wax phase change for temperature reduction, Arab. J. Sci. Eng. (2024) 1–14, https://doi.org/10.1007/s13369-023-08581-3.
[71] Manash Jyoti Deka, Akash Dilip Kamble, Dudul Das, Prabhakar Sharma, Shahadath Ali, Paragmoni Kalita, Bhaskor Jyoti Bora, Pankaj Kalita, Enhancing the performance of a photovoltaic thermal system with phase change materials: Predictive modelling and evaluation using neural networks, Renewable Energy, Volume 224, 2024, 120091, ISSN 0960-1481,Doi: 10.1016/j.renene.2024.120091.
[72] Domenico Mazzeo, Emanuele Ogliari, Andrea Lucchini, Alberto Dolara, Igor Matteo Carraretto, Giampaolo Manzolini, Luigi Pietro Maria Colombo, Sonia Leva,

Integration of photovoltaic modules with phase change materials: Experimental testing, model validation and optimization, Energy, Volume 319, 2025, 134959, ISSN 0360-5442, Doi: 10.1016/j.energy.2025.134959.
[73] A. Sanchez-Brito, F. Cruz-Flores, J. Uriarte-Flores, M. Che-Pan, E. Simá, Dynamic simulation of phase change materials for temperature reduction in photovoltaic panels, Applied Thermal Engineering, Volume 274, Part A, 2025, 126647, ISSN 1359-4311, Doi: 10.1016/j.applthermaleng.2025.126647.
[74] Somchai Jiajitsawat, John Duffy, A portable direct-PV thermoelectric vaccine refrigerator with ice storage through heat pipes, International Solar Energy Conference, 2006, https://www.scopus.com/inward/record.uri?eid=2-s2.0-33845789219&partnerID=40&md5=d5c0b59ccd1c826b278c59a2104e200a.
[75] Somchai Jiajitsawat, John Duffy, A portable direct-PV thermoelectric vaccine refrigerator with ice storage through heat pipes, American Solar Energy Society - Solar 2006: 35th ASES Annual Conf., 31st ASES National Passive Solar Conf., 1st ASES Policy and Marketing Conf., ASME Solar Energy Division Int. Solar Energy Conference, Volume 1, Pages. 242 – 249, https://www.scopus.com/inward/record.uri?eid=2-s2.0-84867965423&partnerID=40&md5=a85c32c3b6d654679e7aeeb2dea8f36e.
[76] Y. Kozak and G. Ziskind, Novel enthalpy method for modeling of PCM melting accompanied by sinking of the solid phase, International Journal of Heat and Mass Transfer, Volume 112, 2017, Pages 568–586, ISSN 0017-9310, Doi: 10.1016/j.ijheatmasstransfer.2017.04.088.
[77] Valerio Lo Brano, Giuseppina Ciulla, Antonio Piacentino, and Fabio Cardona. Finite difference thermal model of a latent heat storage system coupled with a photovoltaic device: Description and experimental validation. Renewable Energy, Volume 68, 2014, Pages 181–193, ISSN 0960-1481, Doi: 10.1016/j.renene.2014.01.043.
[78] V.R. Voller and C. Prakash. A fixed grid numerical modelling methodology for convection-diffusion mushy region phase-change problems. International Journal of Heat and Mass Transfer, Volume 30, Issue 8, 1987, Pages 1709–1719, ISSN 0017-9310, Doi: 10.1016/0017-9310(87)90317-6.
[79] W.D. Bennon and F.P. Incropera. A continuum model for momentum, heat and species transport in binary solid-liquid phase change systems—I. Model formulation. International Journal of Heat and Mass Transfer, Volume 30, Issue 10, 1987, Pages 2161–2170, ISSN 0017-9310, Doi: 10.1016/0017-9310(87)90094-9.
[80] Miao Cui, Chunyun Zhang, Bowen Zhang, Bingbing Xu, Haifeng Peng, and Xiao Wei Gao. Numerical solution of phase change heat transfer problems by effective heat capacity model and element differential method. Journal of Computational Science, Volume 60, 2022, Article 101593, ISSN 1877-7503, Doi: 10.1016/j.jocs.2022.101593.
[81] L.F. Cabeza, A. Castell, C. Barreneche, A. de Gracia, A.I. Fernández, Materials used as PCM in thermal energy storage in buildings: A review, Renewable and Sustainable Energy Reviews, Volume 15, Issue 3, 2011, Pages 1675-1695, ISSN 1364-0321, Doi: 10.1016/j.rser.2010.11.018.
[82] Ye Song, Shaokun Zou, Qichang Dong, Lin Huang, Zihao Song, Hui Yang, Long Shi, A temperature-dependent fire risk assessment framework for solar photovoltaic station, Sustainable Energy Technologies and Assessments, Volume 60, 2023, 103467, ISSN 2213-1388, Doi: 10.1016/j.seta.2023.103467.
[83] M.C. Falvo, S. Capparella, Safety issues in PV systems: Design choices for a secure fault detection and for preventing fire risk, Case Studies in Fire Safety, Volume 3, 2015, Pages 1-16, ISSN 2214-398X, Doi: 10.1016/j.csfs.2014.11.002.
[84] Nikolaos Stathopoulos, George Belessiotis, Petros Oikonomou, Elias Papanicolaou, Experimental investigation of thermal degradation of phase change materials for medium-temperature thermal energy storage and tightness during cycling inside metal spheres, Journal of Energy Storage, Volume 31, 2020, 101618, ISSN 2352-152X, Doi: 10.1016/j.est.2020.101618.
[85] D. Dubert, B. Šeta, J. Massons, Jna. Gavaldà, M.M. Bou-Ali, X. Ruiz, V. Shevtsova, Enhancing PCM thermal management in multi-cycle melting-solidification, International Communications in Heat and Mass Transfer, Volume 157, 2024, 107741, ISSN 0735-1933, Doi: 10.1016/j.icheatmasstransfer.2024.107741.
[86] Pablo Dolado, Ana Lazaro, Jose M. Marin, Belen Zalba, Characterization of melting and solidification in a real-scale PCM–air heat exchanger: Experimental results and empirical model, Renewable Energy, Volume 36, Issue 11, 2011, Pages 2906-2917, ISSN 0960-1481, Doi: 10.1016/j.renene.2011.04.008.
[87] Müslüm Arıcı, Feyza Bilgin, Sandro Nižetić, Agis M. Papadopoulos, Phase change material based cooling of photovoltaic panel: A simplified numerical model for the optimization of the phase change material layer and general economic evaluation, Journal of Cleaner Production, Volume 189, 2018, Pages 738-745, ISSN 0959-6526, Doi: 10.1016/j.jclepro.2018.04.057.
[88] Shiwan Zhou, Wenting Lu, Wenfang Li, Suqi Wang, Forecasting the temperature of a building-integrated photovoltaic panel equipped with phase change material using artificial neural network, Case Studies in Thermal Engineering, Volume 57, 2024, 104355, ISSN 2214-157X, Doi: 10.1016/j.csite.2024.104355.